

# THE METEOROLOGICAL MAGAZINE

Vol. 92, No. 1088, March 1963

---

551.510.61:551.551.5:551.593.12

## STELLAR SCINTILLATION

By J. BRIGGS

**Introduction.**—The stars are seen to scintillate or twinkle, that is, their apparent brightness fluctuates rapidly. To the layman this behaviour is merely intriguing but for the astronomer the effects are a nuisance. The inconstant illumination of the stellar image makes observing more difficult and, at times, the accompanying spreading and jumping of the image is so severe as to cause the abandonment of observations. For this reason the subject has been investigated from time to time and the findings of these investigations have meteorological implications.

To the unaided eye scintillation appears as a brightness variation but in the telescope of the astronomer the intensity variations are less obvious than the blurring and jumping of the image which is partially due to phase scintillation, that is, to phase changes in the incoming light. Both phase and intensity scintillations are manifestations of the same phenomenon. By the eye the frequency of the fluctuations can be estimated as one to 10 cycles per second but the use of light-sensitive instruments of low time-constant reveals fluctuations of between one and 1000 cycles per second.

The intensity of scintillation decreases as the star rises above the horizon which suggests that by far the greater part of the effect is a function of the depth of the earth's atmosphere traversed by the incoming light. Other factors may be involved and, indeed, a physiological explanation was once put forward, but it is now well established that the scintillation is due to local fluctuations in the refractive index of air which, at the wavelengths of visible radiation, depends only on air density and, hence, on air temperature, pressure and water-vapour pressure. For the visible wavelengths the effect of vapour pressure is small in comparison with those of temperature and pressure. As the wavelength increases the refractive index of air ceases to be dependent only on density, and other factors are introduced which increase the effect of vapour pressure, and at radio wavelengths the effect becomes important. Pressure changes are also probably unimportant except for changes on a scale so large and hence so slow that the effects would not be recognized as scintillation. Thus the variation of refractive index which causes the scintillation is mainly due to small-scale temperature fluctuations. These fluctuations are a manifestation of the turbulence of the air and it may be that study of the facts of scintillation can lead to increased knowledge of atmospheric turbulence.

**Stellar shadow patterns.**—The refractive index of air changes, more or less regularly, with variation of time, height and distance but in addition there exist small sudden changes due to convective mixing or to turbulence. These local changes cause small deviations about the mean path of a beam of star-light and two neighbouring beams which have slightly different mean paths will encounter slightly different deviations so that, after passing through a turbulent layer, the two beams will tend to converge or to diverge as they approach the ground. Thus, at some places on the ground an intensification of illumination will be produced whilst other places will have decreased illumination. The result is patchy distribution of relatively light and dark areas which is called the “shadow pattern” of the star. The size of the elements in the shadow pattern is related to the size of the disturbing eddies, and the dominant eddy size will determine the scale of the shadow pattern. Since the atmospheric irregularities are always changing the shadow pattern is in constant movement.

The shadow pattern may be seen if the eye is placed behind a diaphragm in the focal plane of a telescope, pointed toward a bright star, and the eye focused on the objective. If the eye is replaced by a light-sensitive cell connected to suitable magnifying circuits then fairly precise quantitative observations of the shadow pattern are possible.

The arguments of geometrical optics have been used above in accounting for the shadow pattern formation. Theoretical treatments of scintillation based on geometrical optics, or on approximations to wave theory, have been given by several writers, notably Bergmann,<sup>1</sup> Chandrasekhar<sup>2</sup> and van Isacker.<sup>3</sup> These treatments are useful so long as the turbulent elements concerned are large in comparison with the wavelength of light; also the depth of the turbulent layer must not be too big. If the conditions for validity of simple geometrical theory are not satisfied then diffraction effects have to be considered and the turbulent layer must be regarded as a large irregular diffracting screen in the manner first followed by Booker, Ratcliffe and Shinn.<sup>4</sup>

In general the turbulence concerned is mild and the corresponding diffraction “grating” is weak. The problem can then be treated as one in which the shadow pattern is due to interference between the undeviated light, i.e. most of the light, and the deviated light. When the turbulence is more severe and more of the incident light is scattered, then the single scattering approach is no longer tenable and a more complicated multiple scattering theory is required. The single scattering approach has been used by a number of writers notably Ellison,<sup>5</sup> van Isacker,<sup>6</sup> Megaw<sup>7</sup> and Scheffler.<sup>8</sup> Multiple scattering has been treated by van Isacker,<sup>3</sup> Keller<sup>9,10</sup> and by Keller and Hardie.<sup>11</sup>

Using the weak-grating approximation to diffraction theory, an expression can be obtained, see Keller,<sup>12</sup> for the relation between the spectrum function of the amplitudes of refractive index fluctuations and the corresponding function of the amplitude of fluctuations of illumination at the ground, thus:

$$\frac{F(L)}{(\text{mean light intensity})^2} \propto \frac{df(L) \sin^2(\pi z \lambda/L^2)}{\lambda^2}, \quad \dots (1)$$

where  $F(L)$  = spectrum function of the squares of the amplitudes of the Fourier components of the refractive index fluctuations,

$f(L)$  = corresponding function for the illumination fluctuations,

- $L$  = wavelength of the particular component of the shadow pattern,  
 $\lambda$  = wavelength of the light,  
 $z$  = mean height of the turbulent layer,  
 $d$  = thickness of the layer,

The theory assumes the turbulence to be isotropic. This is reasonable since the largest eddies are unlikely to produce effects recognizable as scintillation and the smallest eddies are usually isotropic even if the turbulence as a whole is not.

When  $\pi z \lambda / L^2$  is small the above expression reduces to

$$\frac{F(L)}{(\text{mean light intensity})^2} \propto \frac{d z^2 f(L)}{L^4} \dots (2)$$

This expression is derivable from geometrical theory. The effective value of  $z$  is the distance along the light path between the turbulent layer and the observer and thus increases in proportion to the secant of the zenith distance so that  $\pi z \lambda / L^2$  is not small, and the expression (2) is not valid, for large zenith distances.

Expression (2) shows no dependence on  $\lambda$  which implies that there is little or no colour scintillation for stars near the zenith; this is in accord with observations made by Mikesell, Hoag and Hall<sup>13</sup> and by Protheroe.<sup>14</sup>

Both  $d$  and  $z$  increase in proportion to the secant of zenith angle ( $x$ ). Thus near the zenith, when expression (2) applies, the mean square amplitude of the scintillation should vary as  $\sec^3 \chi$ . If expression (1) applies it may be shown that the mean square amplitude should vary as  $\sec x$ . Observational data have been used to check the expressions in this way, e.g. van Isacker,<sup>6</sup> Protheroe<sup>14</sup> and Scheffler.<sup>8</sup> Good support for the expressions is found although there is a fair amount of scatter.

Using a multiple-scattering theory, van Isacker<sup>3</sup> obtained an expression for the spectrum of the Fourier components in the spatial variation of light intensity in the shadow pattern. This treatment involves a number of approximations and assumes that the turbulent layer is thin so that the light wave is phase-modulated only. It is also necessary to assume that the layer is at a height large in comparison with the size of the largest turbulent element. Keller<sup>10</sup> obtained results which agree with those of van Isacker though avoiding some of the approximations used by van Isacker; on the assumption that the auto-correlation function of the density fluctuations is isotropic and Gaussian, Keller computes spectra of intensity fluctuations in the shadow patterns.

**The relation of scintillation to atmospheric turbulence.**—Although it is well established that atmospheric turbulence is the primary cause of scintillation it is not clear whether the whole atmosphere or only part is involved. The use of ultra-rapid thermometers shows small-scale turbulence to be present at all heights and times in the troposphere and lower stratosphere; it seems reasonable to suppose that all these layers are involved in the production of scintillation. However, it is important to realize that there is a focusing effect involved. This effect is shown in expression (2), where the amplitude of the shadow spectrum produced by a turbulent layer is seen to be proportional to the square of the height of the layer. The focusing effect may be explained by the fact that the convergence, or divergence, of neighbouring light beams which is produced by atmospheric variations is very small so that, if the layer involved is near the ground, then the difference between the beams at the ground is

extremely small and true scintillation is not produced, although some image spreading occurs which is associated with bad astronomical "seeing" conditions. Great heights are ruled out as effective contributors since the mean density decreases exponentially with height.

There is some evidence, e.g. Mikesell,<sup>15</sup> that poor "seeing" and scintillation are not strongly correlated. Indeed it has been shown that conditions in the telescope itself or near that observatory can contribute to poor "seeing". Butler<sup>16</sup> also records that good seeing and haze go together whilst Ellison<sup>17</sup> states that astronomical seeing is usually better on mountain tops. Experience therefore suggests that poor seeing conditions are due to the lower layers of the atmosphere whereas scintillation is due to the layers in the upper troposphere and lower stratosphere. It must be noted too that temperature fluctuations occur most readily when strong wind shear is combined with non-adiabatic lapse rate, conditions most likely to be well developed in the vicinity of inversion layers and of the tropopause.

### **Observational comparisons of scintillation and atmospheric conditions.**

*Size of turbulent element.*—Estimates of the size of the elements in the shadow pattern can be made by comparing the effects of the planets with those of the stars. Since a planet subtends a relatively large angle compared with the turbulent elements then each point of the planet scintillates like a star but the total light remains steady (Ellison and Seddon<sup>18</sup>). Ellison<sup>17</sup> determined the critical angular diameter for production of scintillation by observation of the planets and their satellites and found the average turbulent element to have an angular diameter of about 3 seconds. Variation of the size of the telescope aperture showed the brightness variation to be greatest with apertures of about 7 cm which suggested the shadow pattern elements to be of this order. The size of the real turbulent element does not necessarily equal that of the shadow pattern element, but Ellison found that the amplitude variations did not fall far below the mean amplitude and so indicated a close correspondence between the sizes of the two elements. Keller<sup>10</sup> used data obtained by Protheroe<sup>14</sup> and Scheffler<sup>8</sup> in a quasi-quantitative analysis based on multiple scattering theory. He accounted for the data by taking the turbulent element size to be 5 to 8 cm with a corresponding root mean square temperature fluctuation of 0.1 to 0.4°C. These values corresponded to a layer thickness of 10 to 40 m but root mean square temperature fluctuations of the order of 0.01°C would also have satisfied the data provided the layer thickness was in the region of 2000 to 4000 m. Keller differentiated between the different scales of temperature fluctuations by comparing the values of root mean square temperature changes produced by adiabatic mixing through the relevant layer thicknesses, and in this way rejected the smaller values of temperature fluctuations (and corresponding thicker layers).

*The direction of motion of shadow patterns.*—The movement of the shadow pattern across a telescope may be measured by exposing photographic plates in the focal plane of the telescope. Ellison<sup>17</sup> describes such a method. Hosfeld<sup>19</sup> used increasing time exposures and showed that the recorded pattern tended to elongate with increasing exposure duration thus indicating distinct pattern movement. If the telescope objective is stopped down to a rectangular slit, the directional effect of the shadow pattern is also shown since the frequency of the

scintillation measured varies with the direction of the slit; low-frequency components are favoured when the slit is parallel to the motion and high-frequency components when the slit is normal to the motion. This effect, discovered by Mikesell, Hoag and Hall,<sup>13</sup> was also used by Protheroe<sup>20</sup> who found strong correlation of the pattern direction with that of the wind at 200 mb. Barnhart, Protheroe and Galli,<sup>21</sup> using dual telescopes, made simultaneous readings of the intensity of illumination at two points in the shadow pattern and found similarity of pattern appearance, combined with a time shift, when the two probes were in line with the pattern movement.

*The speed of the shadow patterns.*—The dual probe method of Barnhart, Protheroe and Galli<sup>21</sup> gives the velocity of the pattern movement since the time shift between the two observed patterns can be measured. Comparison of the results with radiosonde winds suggests that the altitude of the pattern-producing layer is above 10,000 feet. The pattern velocity has also been determined by examination of the streaks produced on photographic plates though on some nights the results were indeterminate due, possibly, to motion occurring in several layers moving with different velocities (see Ellison<sup>17</sup>).

*The height of the turbulent layer.*—Correlations between the scintillation and wind velocities at various heights have been reported by a number of workers. In general, the heights of agreement are above 20,000 ft, for example as reported by Gifford and Mikesell,<sup>22</sup> Mikesell,<sup>15</sup> Gifford<sup>23</sup> and Protheroe<sup>20</sup> though Mikesell suggests a correlation with winds at much lower levels, up to 20,000 ft, for the 10 c/sec scintillation. Ellison<sup>17</sup> deduced a height of the turbulent elements of about 2.6 km from their estimated angular diameter of 3 seconds. Barnhart, Protheroe and Galli<sup>21</sup> compared the dual probe measurements of pattern movement with radiosonde winds and found close association for heights within 8000 feet of the tropopause, though it must be observed that on some nights a very wide height range would have given good agreement. By observing the scintillation of double stars Gardiner *et alii*<sup>24</sup> conclude that the 150 c/sec scintillation is produced at heights of 10,000 to 40,000 feet but the 1 to 10 c/sec scintillation is developed as high as 100,000 feet.

The quantitative analysis by Keller,<sup>10</sup> using data by Protheroe<sup>13</sup> and based on the multiple scattering theory, gives a height between 8 and 15 km for the turbulent layer and a corresponding layer thickness of between 10 and 40 m.

Keller<sup>25</sup> also showed that the average spatial autocorrelation function of the shadow pattern is related to the average root mean square deviation of the combined brightness of the star, observed simultaneously by two telescopes. Protheroe<sup>14</sup> simplified this method by using a single telescope of large aperture and an objective diaphragm with two relatively small holes. On the measurements for three nights he deduced shadow pattern movements which agreed closely with the winds at 200 mb as shown by contour charts. Barnhart, Keller and Mitchell<sup>26</sup> developed this autocorrelation method using two telescopes and an automatic correlation computer. They found that on some nights there were several possible altitudes of agreement as regards wind direction and direction of shadow pattern movement but that as regards velocity no more than two altitudes of agreement were possible. Combination of direction and velocity generally gave a unique altitude of agreement between 12 and 14 km (the tropopause varied between 11 and 15 km). The method also indicated spectra of pattern element sizes and showed the dominant turbulent element to be between 15 and 30 cm.

**Summary.**—The experimental evidence strongly suggests that the temporal variations of scintillation at a fixed point are largely due to the translation of fixed shadow patterns across the line of sight. Furthermore, the correlations obtained with wind observations suggest that the important layers are those in the high troposphere and low stratosphere although the temperature fluctuations observed might indicate that all the layers of the troposphere are contributory.

Megaw<sup>7</sup> has suggested that optical and radio measurements are more readily explained by an everchanging multi-layered model than by a few-layered model. It must be noted that on occasions the experimental data fit the winds at several heights and, of course, the winds at different levels are highly inter-correlated. If a multi-layer model were involved it might be expected that a mean wind over a deep section of the atmosphere would correspond to pattern movement; certainly on occasions such a mean wind, excluding surface layers, would fit the data reasonably well.

Temperature fluctuations are usually biggest in inversion layers. It may be that, in general, the amplitude of fluctuation is negligible as regards scintillation and only when the layer is high (for maximum focusing effect) and corresponds to an inversion layer (for greatest amplitude) does the variation of illumination become significant.

The high frequency of the scintillation calls for some comment. On a single-layer theory the observed frequencies correspond to turbulent elements of about 10 cm (for example, if the wavelength of shadow pattern is  $L$ , the frequency is  $f$  and the wind speed at the turbulent layer is  $V$ , we then have  $L = V/f$ ; a reasonable value for  $V$  is 25 m/sec so that if  $f$  is 100 c/sec then  $L = 25$  cm). It is difficult to visualize elements on this scale as having temperature fluctuations as large as the 0.1 to 0.4°C required by single-layer theory. The more probable order of fluctuation of temperature on this scale is 0.01°C. Keller found that this order of fluctuation required a much thicker layer, of thousands rather than tens of metres, but then rejected this solution since adiabatic mixing through such a thick layer produces root mean square temperatures greatly in excess of the prescribed temperature fluctuation. This rejection seems somewhat arbitrary since the size of the eddies causing the temperature fluctuations may be considerably less than the full depth of the turbulent layer. It may be that the turbulent elements are an order or so larger, say one metre or more, and the high frequency of scintillation due partly to the interaction of a limited number of relatively thin turbulent layers.

#### REFERENCES

1. BERGMAN, P. G.; Propagation of radiation in a medium with random irregularities. *Phys. Rev., Lancaster, Pa.*, **70**, 1946, p. 486.
2. CHANDRASEKHAR, S.; A statistical basis for the theory of stellar scintillations. *Mon. Not. R. astr. Soc., London*, **112**, 1952, p. 475.
3. ISACKER, J. VAN; La scintillation des étoiles. Publ. Inst. R. Mét. Belgique, Bruxelles, Series B, No. 8, 1953.
4. BOOKER, H. G., RATCLIFFE, J. A. and SHINN, D. H.; Diffraction from an irregular screen with applications to ionosphere problems. *Phil. Trans., London*, **242**, A, 1950, p. 579.
5. ELLISON, T. H.; The propagation of sound waves through a medium with very small random variations in refractive index. *J. atmos. terr. Phys., London*, **2**, 1952, p. 14.
6. ISACKER, J. VAN; The analysis of stellar scintillation phenomena. *Quart. J. R. met. Soc., London*, **80**, 1954, p. 251.
7. MEGAW, E. C. S.; Interpretation of stellar scintillation. *Quart. J. R. met. Soc., London*, **80**, 1954, p. 248.

8. SCHEFFLER, H.; Astronomische Scintillation und atmosphärische Turbulenz. *Astr. Nachr., Kiel*, **282**, 1955, p. 193.
9. KELLER, G.; Astronomical "seeing" and its relation to atmospheric turbulence. *Air Force Cambridge Research Center, Contract No. AF 19(604)-41, Tech. Rep. 53-15 Cambridge, Mass.*, 1952.
10. KELLER, G.; Stellar scintillation and its relation to atmospheric turbulence. *Air Force Cambridge Research Center, Contract No. AF 19(604)-1409, Sci. Rep. 4., Columbus, Ohio*, 1954.
11. KELLER, G. and HARDIE, R.; Experimental verification of a recently proposed theory of astronomical seeing. *Astr. J., Albany*, **59**, 1954, p. 105.
12. KELLER, G. *et alii*; Investigations of stellar scintillation and the behaviour of telescopic images. *Air Force Cambridge Research Center, Contract No. AF 19(604)-1409, Final Report, Columbus, Ohio*, 1956.
13. MIKESSELL, A. H., HOAG, A. A. and HALL, J. S.; The scintillation of starlight. *J. opt. Soc. Amer., Philadelphia, Pa.*, **41**, 1951, p. 689.
14. PROTHEROE, W. M.; Determination of shadow-pattern structure from stellar scintillation measurements. *J. opt. Soc. Amer., Philadelphia, Pa.*, **45**, 1955, p. 851.
15. MIKESSELL, A. H.; The scintillation of starlight. *Publ. U.S. nav. Obs., Washington*, Second series, **17**, pt. iv, 1955, p. 139.
16. BUTLER, H. E.; Observations of stellar scintillation. *Quart. J. R. met. Soc., London*, **80**, 1954, p. 241.
17. ELLISON, M. A.; Location, size and speed of refractive irregularities causing scintillation. *Quart. J. R. met. Soc., London*, **80**, 1954, p. 246.
18. ELLISON, M. A. and SEDDON, H.; Some experiments on the scintillation of stars and planets. *Mon. Not. R. astr. Soc., London*, **112**, 1952, p. 73.
19. HOSFELD, R.; Comparisons of stellar scintillation with image motion. *J. opt. Soc. Amer., Philadelphia, Pa.*, **44**, 1954, p. 284.
20. PROTHEROE, W. M.; Preliminary report on stellar scintillation. *Air Force Cambridge Research Center, Contract No. AF 19(604)-41, Sci. Rep. 4, Cambridge, Mass.*, 1954.
21. BARNHART, P. E., PROTHEROE, W. M. and GALLI, J.; Direct observation of element motion in stellar shadow patterns. *J. opt. Soc. Amer., Philadelphia, Pa.*, **46**, 1956, p. 904.
22. GIFFORD, F. and MIKESSELL, A. H.; Atmospheric turbulence and the scintillation of starlight. *Weather, London*, **8**, 1953, p. 195.
23. GIFFORD, F.; The height of scintillation-producing disturbances. *Bull. Amer. met. Soc., Lancaster, Pa.*, **36**, 1955, p. 35.
24. GARDINER, A. J. *et alii*; Optical studies of atmospheric turbulence. *Air Force Cambridge Research Center, Contract No. AF 19(604)-953, Final Report, Flagstaff, Arizona*, 1956.
25. KELLER, G.; The relation between the structure of stellar shadow pattern and stellar scintillation. *J. opt. Soc. Amer., Philadelphia, Pa.*, **45**, 1955, p. 845.
26. BARNHART, P. E., KELLER, G. and MITCHELL, W. E.; Investigation of upper air turbulence by the method of analyzing stellar scintillation shadow patterns. *Air Force Cambridge Research Center, Contract No. AF 19(604)-1954, Final Report, Columbus, Ohio*, 1959.

551-557-33:551-557-5

## WINDS AT THE 200 MB LEVEL OVER THE TROPICS AND SUB-TROPICS DURING THE SEASONS OF MONSOON CHANGE

By J. G. LOCKWOOD, Ph. D.

**Introduction.**—In Geophysical Memoirs No. 103 (Upper Winds over the World)<sup>1</sup> mean upper air charts were published for the midseason months, January, April, July and October. In temperate latitudes the changes in the upper flow patterns (except at very high levels) between the midseason months are gradual, and it is therefore possible to obtain approximate means for the remaining months by simple interpolation. There are, however, two complete reversals of the 200 mb flow during the year in parts of the tropics. This can be seen by comparing the 200 mb average wind charts for January and July in Geophysical Memoirs No. 103. These reversals normally occur in May or June and in October, and take place within a period of a few weeks. They coincide with the advance in May and the retreat in October of the south-west monsoon over southern Asia. Hence it is impossible in the tropics to obtain mean winds for these transitional months by simple interpolation between the charts for midseason months.

To supplement Geophysical Memoirs No. 103, mean charts have been prepared to cover the two transitional periods in the tropics. Because the changes are completed in periods of less than one month it is desirable to prepare these charts for ten-day periods. The reversal of the 200 mb flow is most marked over Ethiopia and Sudan, and southern Asia. Over the tropical central Pacific and South America winds appear to be normally light, but there is a serious lack of data for these areas. The charts are limited to the area  $20^{\circ}\text{W}$ – $180^{\circ}\text{E}$ ,  $40^{\circ}\text{N}$ – $40^{\circ}\text{S}$ , within which the wind reversal is most prominent.

The mean charts in Geophysical Memoirs No. 103, were mainly based on the five-year period 1949–53. At most tropical stations, regular upper air observations to 200 mb were only started during the late 1950's. Even during this period many ascents failed to reach 200 mb. Therefore it was decided to use the seven-year period 1954–60 for computing the means for the present charts. This allowed an adequate sample of observations to be obtained from many tropical stations.

The mean wind charts were mainly constructed from the wind observations. Ten-day mean 200 mb contour charts were also constructed, and these were taken into account when constructing the mean wind charts except within about  $15^{\circ}$  of the equator. There was some difficulty in drawing reasonable streamline-isotach patterns over equatorial regions. This was partly due to a lack of data and partly to the charts covering a transition which may vary in date from year to year.

**The transition in May and June.**—The main features of the 200 mb wind fields shown on the ten-day average charts for May and June (Figures 1 to 6) are as follows:

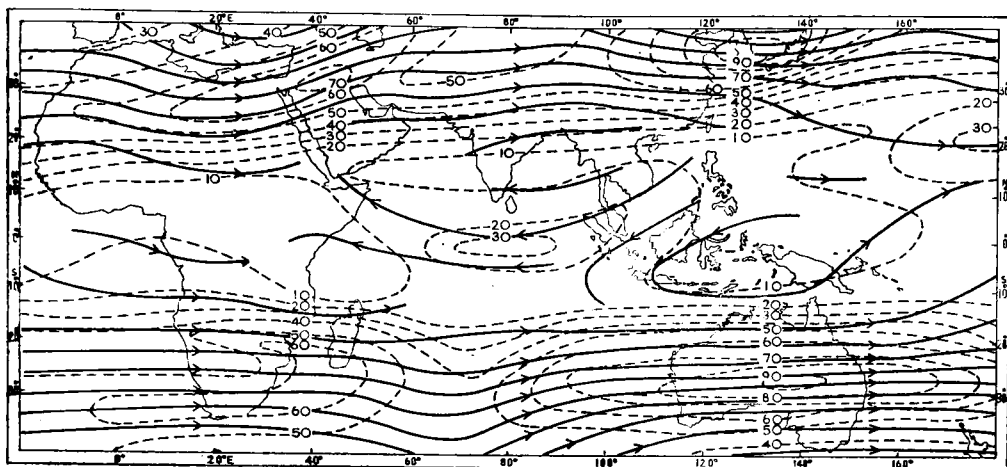
- (a) the northern hemisphere subtropical westerly current,
- (b) the equatorial easterly currents and
- (c) the southern hemisphere subtropical westerly current.

There is one small scale feature shown on the charts:

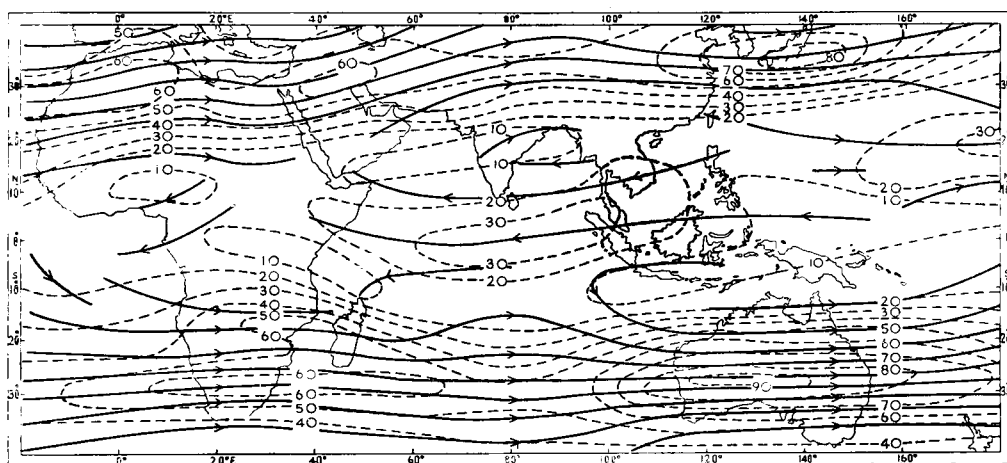
- (d) the Wake Island–Johnston Island westerly current.



FIGURE 1—AVERAGE 200 MB WINDS (KT), 1–10 MAY 1954–60  
Isotachs are shown by broken lines and streamlines by continuous lines.



**FIGURE 2—AVERAGE 200 MB WINDS (KT), 11-20 MAY 1954-60**  
Isotachs are shown by broken lines and streamlines by continuous lines.



**FIGURE 3—AVERAGE 200 MB WINDS (KT), 21-30 MAY 1954-60**  
Isotachs are shown by broken lines and streamlines by continuous lines.

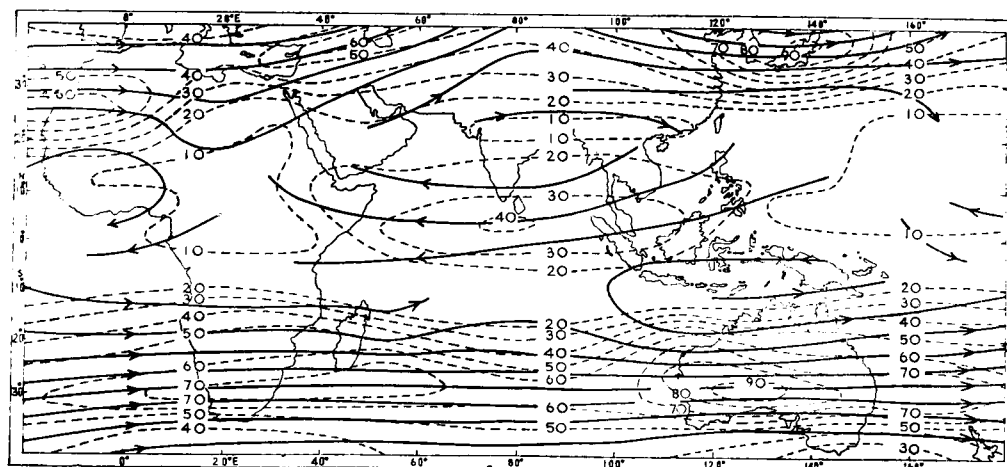


**FIGURE 4—AVERAGE 200 MB WINDS (KT), 31 MAY-9 JUNE 1954-60**  
Isotachs are shown by broken lines and streamlines by continuous lines.

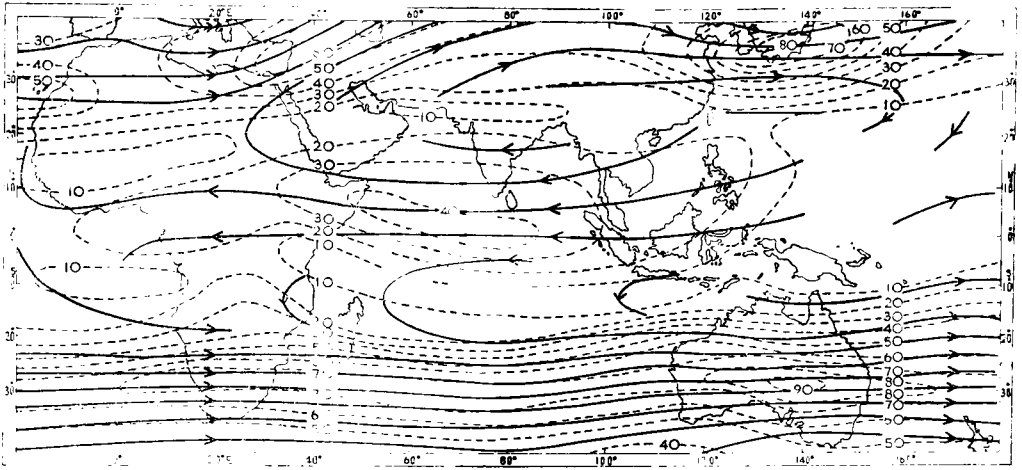


FIGURE 5—AVERAGE 200 MB WINDS (KT), 10-19 JUNE 1954-60  
Isotachs are shown by broken lines and streamlines by continuous lines.

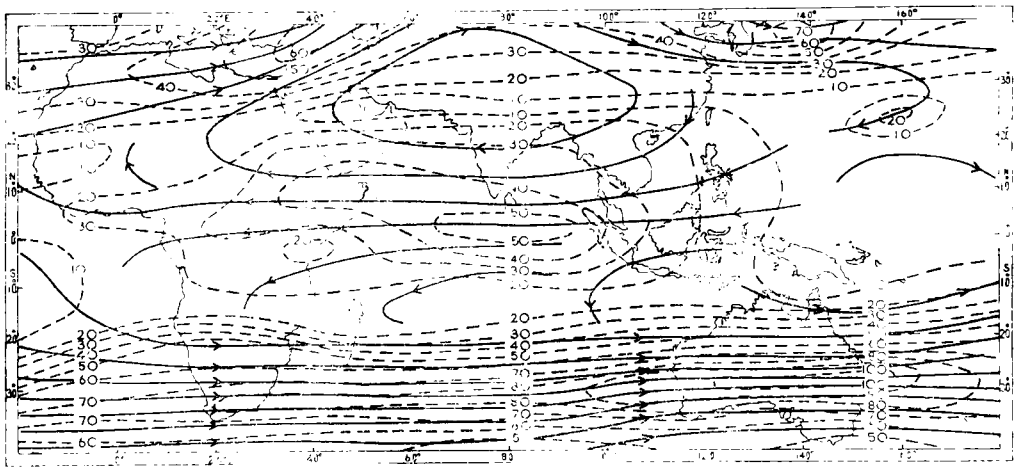


FIGURE 6—AVERAGE 200 MB WINDS (KT), 20-29 JUNE 1954-60  
Isotachs are shown by broken lines and streamlines by continuous lines.

**The northern hemisphere subtropical westerly current.**—This current extends from North Africa to the central Pacific throughout the period. It is divided into two sections with high average wind speeds, one centred over North Africa and the Middle East, and the other over Japan. At the beginning of May (Figure 1) the western maximum, represented by the isopleth for 80 knots, extends from the western Sahara to Iran. For most of May the jet axis continues with the same alignment but the speed decreases, especially over Africa. During June this maximum moves north-west to Asia Minor, with unchanging speed.

The maximum of the subtropical westerly current over Japan undergoes little change in position during May and June. It is associated at first with high average wind speeds, sometimes above 100 knots in the centre. The westward extent of the jet maximum across China is uncertain.

It was first demonstrated by Yin (1949)<sup>2</sup> that the “burst” of the Indian south-west monsoon is connected with the disintegration of the subtropical jet stream over northern India, and the formation of a new jet to the north of the

central Asiatic highlands. Graphs of the daily 200 mb zonal wind components at New Delhi and Jodhpur are reproduced in Figure 7. The disintegration of the jet at these two stations is indicated, except in 1956, by the decreasing values of the zonal components. In 1956 the westerly jet left north-west India before 1 May. The date (see Table I) of the disintegration of the westerly jet over India varies within a period of about six weeks.

TABLE I—LAST FIVE-DAY PERIOD IN SPRING WITH A 200 MB WESTERLY JET\*  
OVER NORTH INDIA

Year	Pentad
1955	21-25 May
1956	Before 1 May
1957	21-25 May
1958	5-9 June
1959	16-20 May

\* Winds in core above 60 kt.

**The equatorial easterly currents.**—At the beginning of May there are weak easterly winds in equatorial regions over the eastern part of the Indian Ocean and over equatorial Africa. These currents expand rapidly, so that by the end of June they extend from West Africa to the Philippines. Over northern Africa and southern Asia, they spread northwards into areas previously occupied by the southern part of the subtropical westerly current, thus causing a complete reversal of the 200 mb winds. This is shown, for example, by the 200 mb wind records from Khartoum (Figure 7) and Aden (Table II).

TABLE II—DATES OF ARRIVAL OF THE EASTERLY JET AT 200 MB OVER ADEN AND KHARTOUM FOR YEARS 1954-60

Station	Year	Date of last observation with a westerly component	Last five-day period with a mean westerly component	First five-day period with a mean easterly component above ten knots
Aden	1954	29 May	6-10 May	31 May-4 June
	1955	31 May	1-5 May	6-10 May
	1956	12 May	Before 1 May	16-20 May
	1957	8 June	21-25 May	26-30 May
	1958	31 May	Before 1 May	1-5 May
	1959	21 May	11-15 May	26-30 May
	1960	15 May	11-15 May	16-20 May
Khartoum	1954	6 June	26-30 May	10-14 June
	1955	6 June	31 May-4 June	10-14 June
	1956	25 May	6-10 May	26-30 May
	1957	18 June	26-30 May	20-24 June
	1958	11 June	5-9 May	15-19 June
	1959	3 June	21-25 May	10-14 June
	1960	13 June	5-9 June	15-19 June

In May and June the easterly currents spread northwards and replace the westerlies at Khartoum and Aden. The dates of their arrival at these two stations are tabulated in Table II. Three different criteria are used, the date of the last observation with a westerly component, the last five-day period with a mean westerly component and the first five-day period with a mean easterly component above 10 knots. The last normally occurs at Aden in mid-May and at Khartoum in mid-June.

**The southern hemisphere subtropical westerly current.**—Between 10°S and 40°S a westerly current covers the whole sector included in the mean charts. Because of a lack of data the detailed features of this current are obscure, except over Australia and South Africa. A jet maximum is centred over

Australia at the beginning of May; this remains nearly constant in position but slowly increases in strength towards the end of June. The westerly current over southern Africa slowly increases in strength throughout May and June.

**The Wake Island–Johnston Island current.**—This is a small westerly current which flows over the central Pacific (about  $180^{\circ}\text{E}$ ,  $18^{\circ}\text{N}$ ). On the average chart for the first decade in May, the speed in the centre of the current is shown as about 65 knots. The current decreases in strength and moves east during May. At the beginning of June it has moved east of longitude  $180^{\circ}$ .

**The changes in the flow pattern during May and June.**—Sutcliffe and Bannon (1954)<sup>3</sup> demonstrated, for the years 1948 to 1953, a time-relationship between the shift of the 200 mb winds from west to east over Aden and Bahrain, the ending of the polar tropopause over Habbaniya and the onset of the south-west monsoon at the Malabar coast of India. Yeh Tu-Cheng, Dao Shih-Yen and Li Mei-Tsuin (1958)<sup>4</sup> have claimed to show that there is an abrupt change in the pattern of the upper tropospheric circulation over the northern hemisphere in June.

In Figure 7 are reproduced graphs of the daily 200 mb zonal winds at Jodhpur, New Delhi and Khartoum. The dates of the start of the south-west monsoon on the Malabar coast (as published by the Indian Meteorological Department<sup>5</sup>) are also noted. In some years the south-west monsoon reached the Malabar coast and then became stationary, or even retreated, and did not start to advance across India until a later date. In these cases two dates are marked. The former is the date of the first advance across the Malabar coast, the latter the start of the true advance across India.

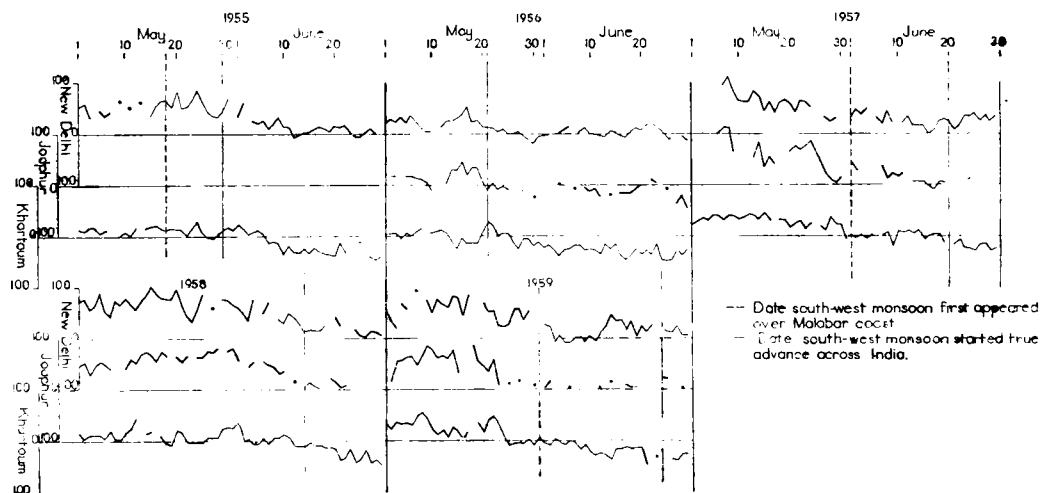


FIGURE 7—DAILY 200 MB ZONAL COMPONENTS (KT) DURING MAY AND JUNE 1955-59, AT NEW DELHI, JODHPUR AND KHARTOUM

Westerly components above the axes, easterly components below the axes.

Figure 7 indicates that in general the strong zonal winds (above 60 knots) associated with the subtropical jet stream left New Delhi and Jodhpur before the start of the main advance of the south-west monsoon across India. In 1955, the ceasing of the strong zonal winds at New Delhi coincided with the start of the main advance of the monsoon.

An inspection of Figure 7, also shows that the main 200 mb easterlies arrived at Khartoum after the start of the south-west monsoon on the Malabar coast. This is in accord with the findings of Sutcliffe and Bannon<sup>3</sup> concerning Aden.

The significant changes in the 200 mb flow patterns during May and June may be considered as taking place in the following order:

- (a) The first notable change is the movement of the high wind speeds associated with the subtropical jet from the southern to the northern side of the highlands of central Asia.
- (b) After this change has taken place, the equatorial easterly current expands rapidly northwards, eastwards, and westwards from the central Indian Ocean across southern Asia, central Africa and the western Pacific.
- (c) Some time after the subtropical jet has left India, and before the 200 mb easterlies become definitely established at Khartoum, the south-west monsoon reaches the Malabar coast of India.

**The transition in October.**—The main features of the average wind charts for May and June were noted earlier. Except for the Wake Island–Johnston Island westerly current, the same main features are found on the average wind charts for October (Figures 8 to 11).

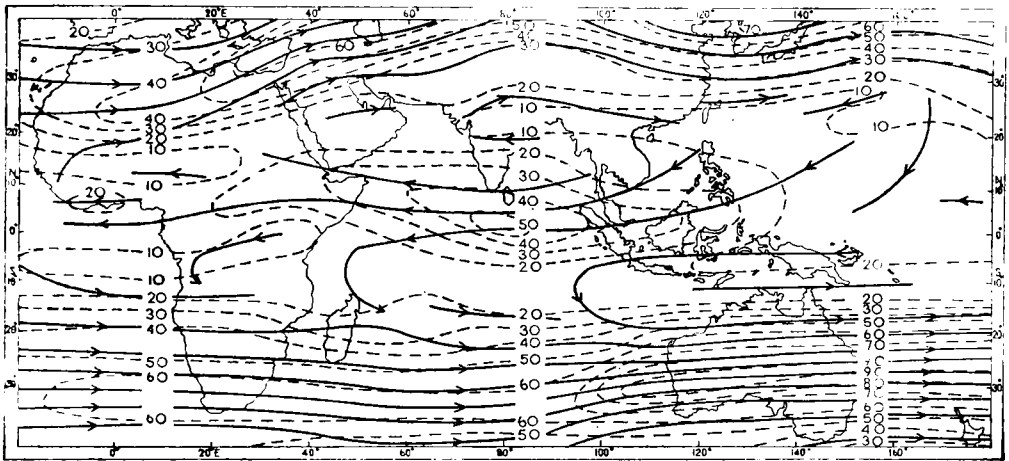


FIGURE 8—AVERAGE 200 MB WINDS (KT), 23 SEPTEMBER–2 OCTOBER 1954–60  
Isotachs are shown by broken lines and streamlines by continuous lines.

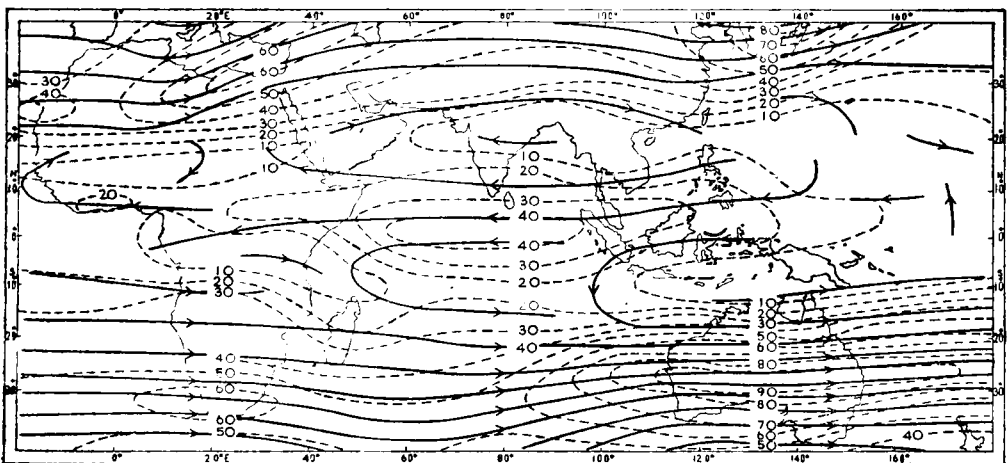


FIGURE 9—AVERAGE 200 MB WINDS (KT), 3–12 OCTOBER 1954–60  
Isotachs are shown by broken lines and streamlines by continuous lines.

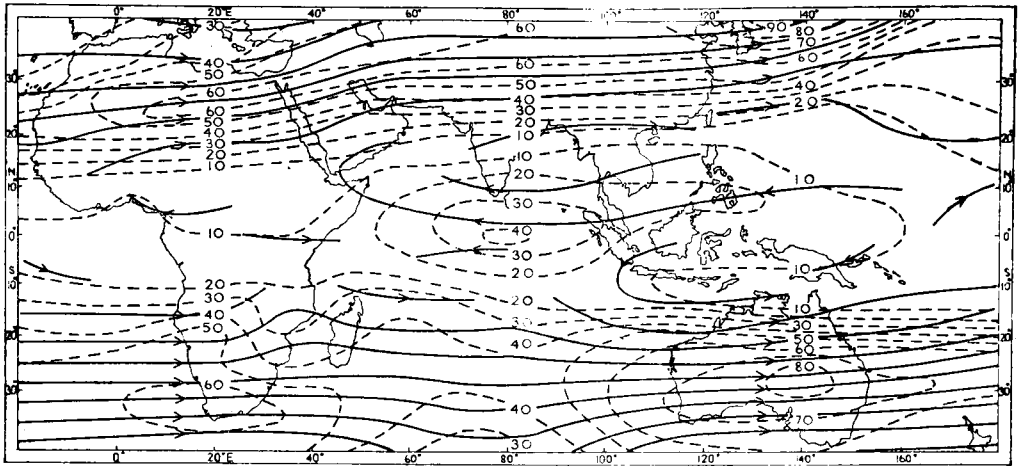


FIGURE 10—AVERAGE 200 MB WINDS (KT), 13-22 OCTOBER 1954-60  
Isotachs are shown by broken lines and streamlines by continuous lines.

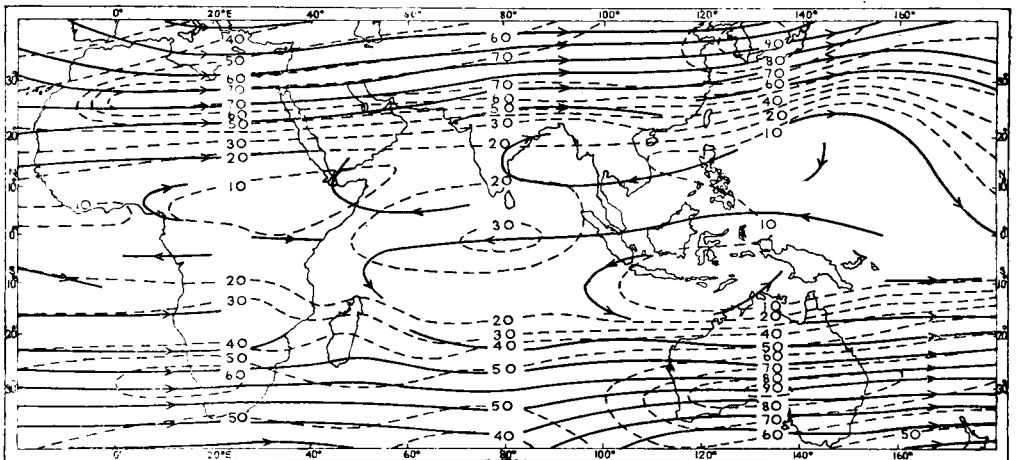


FIGURE 11—AVERAGE 200 MB WINDS (KT), 23 OCTOBER-1 NOVEMBER 1954-60  
Isotachs are shown by broken lines and streamlines by continuous lines.

**The northern hemisphere subtropical westerly current.**—The maximum of the subtropical current is represented by a 50-knot isopleth over Asia Minor on the 200 mb average wind chart for July in Geophysical Memoirs No. 103.<sup>1</sup> Two areas of maximum speed are shown on the average wind chart for 23 September to 2 October (Figure 8), one over the Near East and the other over Japan. The first, represented by the 60-knot isopleth, remains in approximately the same position as the July maximum until the first decade in October. On the chart for the second decade in October (Figure 10), the maximum over the Near East has moved south, and the 60-knot isopleth now encloses an area from the central Sahara to Japan. The chart for the last decade in October (Figure 11) shows the western section of the current roughly in the January position over North Africa, with winds above jet-stream limits (60 knots) over northern India.

Graphs of the daily 200 mb zonal wind components at New Delhi and Jodhpur are reproduced in Figure 12. The dates<sup>5</sup> of the final

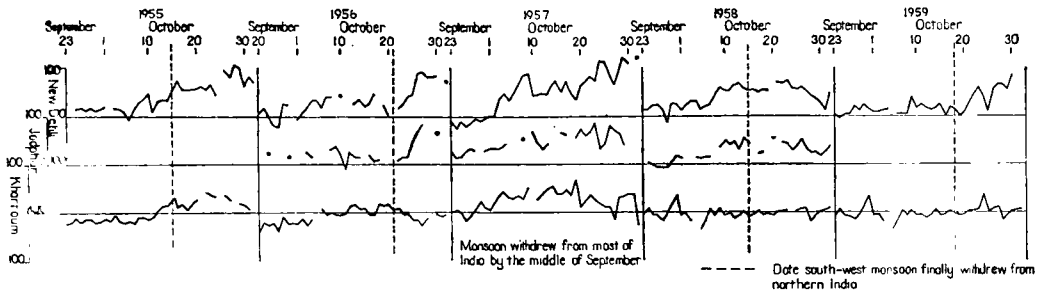


FIGURE 12—DAILY 200 MB ZONAL COMPONENTS (KT) DURING OCTOBER 1955-59, AT NEW DELHI, JODHPUR AND KHARTOUM

Westerly components above the axes, easterly components below the axes.

retreat of the south-west monsoon from northern India are also noted. Except in 1958, strong zonal winds (above 60 knots) associated with the subtropical jet did not become established at New Delhi until after the retreat of the south-west monsoon. In October 1958, the first zonal components above 60 knots at New Delhi occurred a few days before the south-west monsoon left northern India. The relatively sudden increases in the zonal wind speeds at New Delhi and Jodhpur, as the subtropical current forms over northern India, are noteworthy.

The zone of maximum speeds over Japan undergoes little change in position during October. The maximum average speed slowly increases from about 75 knots at the end of September to 95 knots at the end of October.

**The equatorial easterly currents.**—At the end of September (Figure 8), the equatorial easterly currents extend from West Africa to the western Pacific and reach north to central India and southern Saudi Arabia. This is a smaller area than that covered by the currents on the July average chart.<sup>1</sup> During October the area covered by the currents decreases, until at the end of October they are mostly contained between longitudes 55°E and 135°E, with the main current over the Indian Ocean to the south of Ceylon. The disintegration of the equatorial currents during October is not as sudden as their formation in May. In May and June there are marked reversals of the 200 mb winds at stations on the border of the growing equatorial currents. These reversals occur again in October, but they are very much less marked than those occurring in May. Graphs of the daily 200 mb zonal components at Khartoum are reproduced in Figure 12; these illustrate the vague change which takes place at a typical station in October.

**The southern hemisphere subtropical westerly current.**—Between 10°S and 40°S a westerly current covers the average charts for October (Figures 8 to 11). At the end of September there is a wind maximum, indicated by the 90-knot isopleth, over Australia. During October the position of the maximum remains the same, but the wind speed decreases. Over southern

Africa the westerly winds extend slowly north during October, reaching Nairobi by the middle of the month. In November Nairobi had a mean wind of  $264^{\circ}/10$  knots (1948–55).<sup>6</sup>

**Conclusions.**—Over the tropics and subtropics from Africa to the western Pacific, the 200 mb flow patterns can be divided on a climatological scale into two general types. One flow pattern dominates from November to April, and the other from June to September. The average wind charts for January and July in Geophysical Memoirs No. 103,<sup>1</sup> show the two basic flow patterns at their respective greatest developments. The changes in the 200 mb flow pattern in May and June appear to take place in a definite sequence. The October transition is less distinct, but it is still possible to find some order in the sequence of events. The main 200 mb easterly current leaves Khartoum in North Africa before the south-west monsoon retreats from northern India. The south-west monsoon normally retreats from northern India before winds of jet-stream strength (above 60 knots) appear at New Delhi. This would appear to be the reverse of the sequence of events occurring in May and June.

#### REFERENCES

1. HEASTIE, H. and STEPHENSON, P. M.; Upper winds over the world. *Geophys. Mem., London*, **13**, No. 103, 1960.
2. YIN, M. T.; A synoptic-aerologic study of the onset of the summer monsoon over India and Burma. *J. Met., Lancaster, Pa.*, **6**, 1949, p. 393.
3. SUTCLIFFE, R. C. and BANNON, J. K.; Seasonal changes in upper-air conditions in the Mediterranean–Middle East Area. Scientific Proceedings of the International Association of Meteorology, Rome, 1954.
4. YEH TU-CHENG, DAO SHIH-YEN and LI MEI-TSUIN; The abrupt change of circulation over northern hemisphere during June and October. Institute of Geophysics and Meteorology, Academia Sinica, *Acta Met. Sinica, Peking*, **29**, 1958, pp. 249–263.
5. India Meteorological Department, Poona; *Indian Journal of Meteorology & Geophysics*, Vol. 5-12, 1954–61.
6. East African Meteorological Department; Upper air data for Nairobi, 1948–55. 1960.

551.501.45:551.573:681.14

## A COMPUTER PROGRAMME FOR THE CALCULATION OF MEAN RATES OF EVAPORATION USING PENMAN'S FORMULA

By C. P. YOUNG, B.Sc.

(Road Research Laboratory, Department of Scientific and Industrial Research)

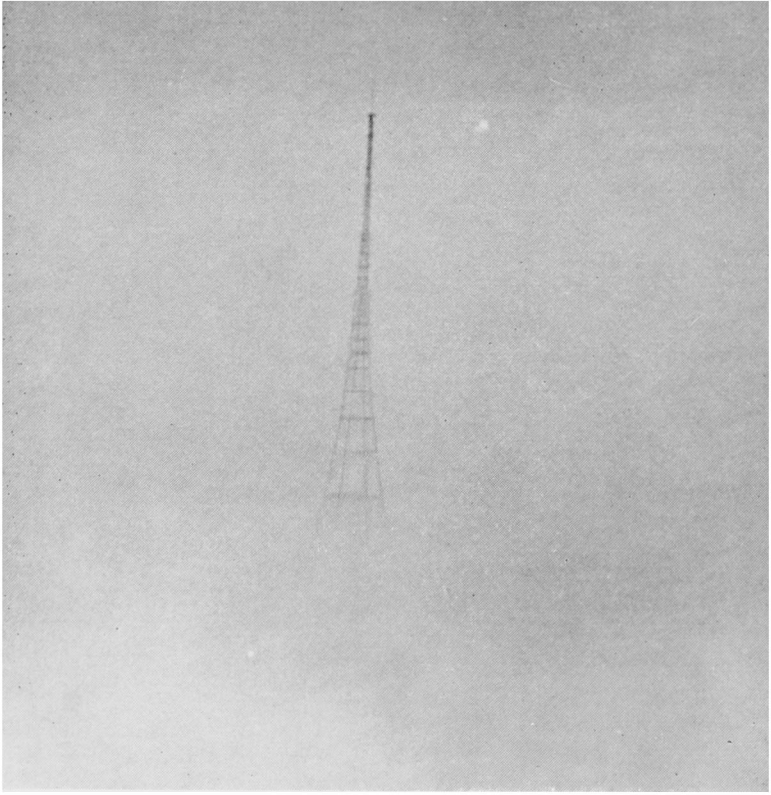
**Summary.**—In hydrological studies estimates of rates of evaporation have to be made from meteorological data, and Penman's formula is used for this purpose at the Road Research Laboratory. A programme for a Ferranti 'Pegasus' computer has been developed by means of which rates of evaporation can be calculated rapidly from the meteorological data. Taking into account the time taken to punch the data on paper tapes, an individual rate of evaporation can be calculated in half a minute.

**Introduction.**—As part of the programme of research into the design of drainage structures for motorways, investigations are being made of the rates of flow in the longitudinal drains of the carriageways and in the culverts beneath the motorways that provide lateral drainage for small natural catchments. Both investigations require a knowledge of rates of evaporation which are to be estimated using the formula devised by Penman.<sup>1, 2</sup>

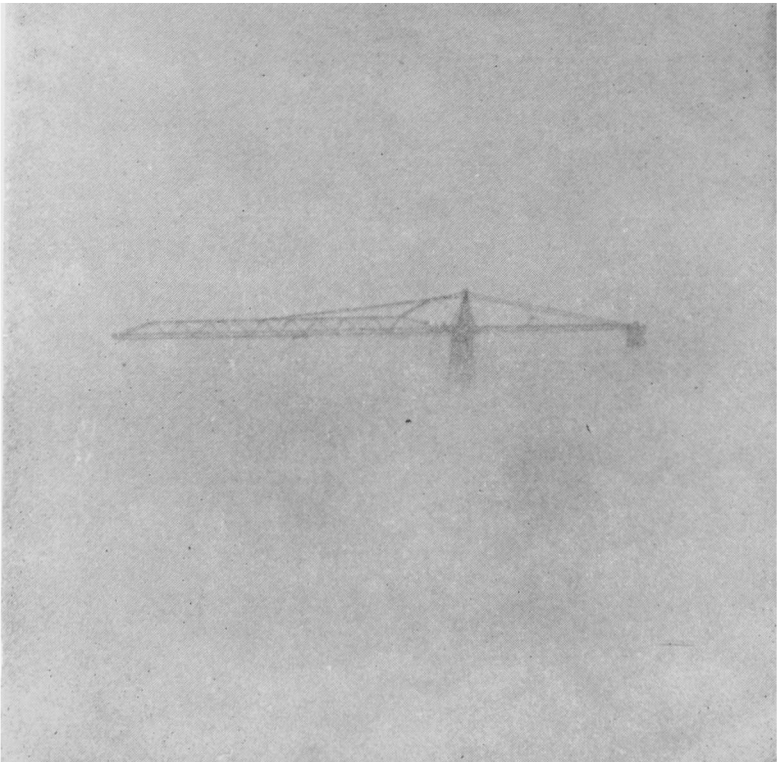


*Crown copyright*

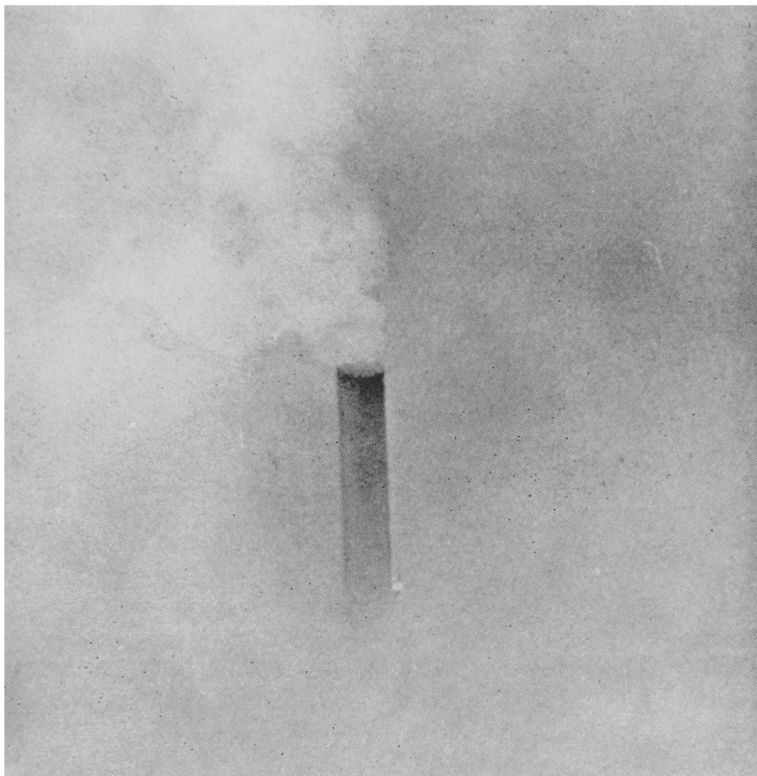
THE METEOROLOGICAL RESEARCH FLIGHT BUILDING AT FARNBOROUGH



*Reproduced by courtesy of Daily Express.*



*Reproduced by courtesy of Daily Express.*



*Reproduced by courtesy of Daily Express.*

#### PHOTOGRAPHS OF THE LONDON FOG, 3-7 DECEMBER 1962

Fog developed over much of south-east England, including the London area, on the evening of Monday 3 December, gradually becoming denser on the following day with visibilities down to 10 yards or less in places, especially in the evening. There was some temporary improvement in most places on Wednesday, mainly during the day, and again on Thursday, but visibility was less than 10 yards in many places on Thursday evening. On the morning of Friday 7 December visibility improved and by evening the fog had cleared over the whole of Greater London.

The top of the fog was between 300 and 400 feet above the Thames and such places as Crystal Palace and the top of Shell building were above the fog at times. The photograph (top left) shows the television mast at Crystal Palace, while the crane (bottom left) is sited on the south bank of the Thames.

This fog period, though shorter, was in many ways similar to the bad fog of 4-9 December 1952. Visibilities in 1952 were somewhat less and the really dense fog (visibility less than 20 yd) was more widespread and persistent. The fog top of 300 to 400 feet was similar in the two cases but temperatures near the ground in low-lying areas of Greater London were about 1°C lower (night minima around minus 6°C) in the 1962 fog than in 1952. Temperatures increased rapidly with height in both cases and reached 4°C or more on hill tops near London.

Fog occurred in most parts of England during the period of London fog in 1962 but, as in the 1952 episode, it was neither as persistent nor as dense in other regions as in the London area.

To face p 85]



*Crown copyright*

THE METEOROLOGICAL RESEARCH FLIGHT BUILDING AT FARNBOROUGH

Penman's formula is to be used for these investigations because it takes into account most of the physical factors involved in evaporation from natural surfaces. To reduce the effort required in the calculations, a programme has been developed for use with a Ferranti 'Pegasus' computer. The development of this programme is described.

**The Penman formula.**—This formula estimates  $E$ , the hypothetical rate of evaporation, as

$$E = \left( \frac{\Delta}{\gamma} H + E_a \right) / \left( \frac{\Delta}{\gamma} + 1 \right) \text{ mm day}^{-1}, \quad \dots (1)$$

where  $E_a = 0.35 (e_a - e_d) \left( 1 + \frac{u_2}{100} \right) \text{ mm day}^{-1}, \quad \dots (2)$

$\Delta$  = the slope of the saturation vapour pressure curve for water at a mean air temperature  $T_a$ ,

$\gamma$  = the constant of the wet- and dry-bulb hygrometer equation,

$H = A - B$ , the net radiation at the earth's surface ( $\text{mm day}^{-1}$ ),

$A = R_a (1 - r) (0.18 + 0.55 n/N)$ , the short-wave incoming radiation ( $\text{mm day}^{-1}$ ), ... (3)

$B = \sigma T_a^4 (0.56 - 0.092\sqrt{e_d}) (0.10 + 0.90 n/N)$ , the long-wave outgoing radiation ( $\text{mm day}^{-1}$ ), ... (4)

$R_a$  = the theoretically calculable amount of radiation received at the earth's surface in the absence of an atmosphere, expressed in evaporation units,

$r$  = the reflexion coefficient,

$n/N$  = the ratio of actual to possible hours of sunshine,

$\sigma T_a^4$  = the theoretical black-body radiation at a mean air temperature  $T_a$ ,

$e_a$  = the saturation vapour pressure of water at a mean air temperature  $T_a$ ,

$e_d$  = the saturation vapour pressure of water at dew-point or the actual vapour pressure at a mean air temperature  $T_a$ ,

$u_2$  = the mean daily wind speed ( $\text{mile day}^{-1}$ ) at a height of 2 metres.

If the reflexion coefficient  $r$  in equation (3) is given the value 0.25,<sup>2</sup> then equation (1) gives, directly,  $E = E_T$ , the potential rate of evapotranspiration from an extended short green crop.

**Tabulation of data.**—To calculate  $E$  for a given locality six basic parameters must be known. These are (i) latitude, (ii) time of year, (iii) actual hours of sunshine, (iv) the mean air temperature, (v) the mean vapour pressure and (vi) the mean daily wind speed.

Instruments are available which can measure either the net radiation received at the earth's surface,  $H$  in equation (1), or the total incoming radiation,  $A$  in equation (3). Readings from these instruments can be used to improve the accuracy of the estimate of the rate of evaporation. If measurements of  $H$  are known, some of the basic parameters need not be given. Table I shows the basic parameters needed depending upon the instruments available.

TABLE I—PARAMETERS NEEDED TO CALCULATE RATES OF EVAPORATION

	Latitude	Time of year	Mean daily values				
			Radiation Incoming Net	Sunshine hours	Air temperature	Vapour pressure or relative humidity	Wind speed
No radiation instruments	*	*		*	*	*	*
Incoming radiation readings available	*	*	*	*	*	*	*
Net radiation readings available			*		*	*	*

The three methods of using the programme are listed in Table I in order of increasing accuracy of the estimate of the rate of evaporation. When measurements of incoming radiation are available the accuracy of the estimate can be improved, but it is still necessary to know the appropriate latitude and time of year. If the net radiation is known, air temperature, vapour pressure and wind speed are the only other parameters needed to estimate the rate of evaporation.

For the purpose of the programme the units of the basic parameters are as follows:

- (i) Latitude; degrees and decimals of a degree, with a negative sign for southerly latitudes.
- (ii) Time of year; either as a month or as the sun's mean daily declination in degrees and decimals of a degree, with a negative sign for southerly declinations.
- (iii) Radiation readings; mean daily values in calories.
- (iv) Sunshine hours; mean daily values in hours.
- (v) Air temperature; mean daily value either in °C or °F.
- (vi) Vapour pressure; either as the mean daily value in millibars or as the mean daily relative humidity expressed as a percentage.
- (vii) Wind speed; mean daily value in miles per day at a height of 2 metres.

**Calculation of dependent variables.**—The programme has been designed so that all the variables dependent upon the basic data are calculated directly, avoiding the use of ancillary tables and graphs. There are four dependent variables involved:

- (i)  $R_a$ , the theoretical amount of radiation received at the earth's surface in the absence of an atmosphere; this is calculated from the formula:

$$R_a = \frac{1440R}{59\pi} (h \sin L \sin D + \sin h \cos L \cos D) \text{ mm day}^{-1}, \quad \dots (5)$$

where

$L$  = latitude,  
 $D$  = sun's mean daily declination,  
 $R$  = the solar constant (usually taken as  $1.94 \text{ cal cm}^{-2} \text{ min}^{-1}$ ) and  
 $h = \cos^{-1} \tan L \tan D$ , . . . (6)  
 angles  $L$  and  $D$  being measured in radians.

Equation (5) neglects small effects such as the eccentricity of the earth's orbit.

(ii)  $N$ , the possible hours of sunshine; this value is found from equation (6) and is given by

$$N = \frac{24h}{\pi} \text{ hours.} \quad \dots (7)$$

(iii)  $e_a$ , the saturation vapour pressure of water at an air temperature  $T_a$ ; this is given by the formula

$$e_a = \exp \left[ \frac{47.226 - 6463}{(273 + T_a)} - 3.927 \ln (273 + T_a) \right] \text{ mm of mercury} \quad (8)$$

(iv)  $\Delta$ , the slope of the saturation vapour pressure curve at an air temperature  $T_a$ ; this is given by differentiating equation (8), thus

$$\Delta = \frac{e_a}{(273 + T_a)} \left[ \frac{6463}{(273 + T_a)} - 3.927 \right]. \quad \dots (9)$$

The constants in equations (8) and (9) were determined from a multiple correlation analysis of values tabulated by Kaye and Laby<sup>3</sup> of the saturation vapour pressure of water between  $0^\circ\text{C}$  and  $40^\circ\text{C}$ .

**The programme.**—The part of the programme concerned with data input has been designed to accept data punched on paper tape in normal units without any scaling or conversion being necessary, the data being preceded by an identifying code letter. The programme has been arranged so that if any items of the basic data are constant for a series of calculations, those items need only be punched on the data tape at the start of the series. A facility for the computation of mean values from daily values is incorporated in the main computer programme. Once the data has been read by the computer, the rate of evaporation is calculated in either millimetres or inches per day.

If the reflexion coefficient  $r$  in equation (3) is given the value  $0.05^1$  then equation (1) gives  $E = E_0$ , the hypothetical rate of evaporation that would take place from an extended sheet of open water.  $E_0$  may be multiplied by a seasonal factor  $f$  to convert  $E_0$  to  $E_T$ , the potential rate of evapotranspiration from a short green crop. If  $r$  is given the value  $0.25$ ,<sup>2</sup> then equation (1) gives  $E_T$  directly. The value of  $r$  in equation (3) can be easily changed in the programme from  $0.25$  to  $0.05$  to give  $E_0$ . If  $r$  is changed to give  $E_0$  in equation (1), the appropriate seasonal factor  $f$  should be specified. The programme will then punch out both  $E_0$  and  $E_T (= f.E_0)$ .

The values of the constants in the cloudiness terms ( $0.18 + 0.55n/N$ ) and ( $0.10 + 0.90 n/N$ ) of equations (3) and (4) can be changed, if desired, to suit local conditions.

Figure 1 shows the data as they would be punched to calculate the mean daily rate of evaporation for each month of the year and Figure 2 shows the results obtained from these data. Using the programme in its longest form, the time taken to punch the data for the calculation of 84 individual rates of evaporation was 40 minutes and the time taken for the actual calculations was 2 minutes.

```

N
UXBRIDGE YEAR 1954                               Title copied to results tape

LAT51.5                                           Latitude constant for series

JAN TF37.9 E6.6 S2.13 W171 L
FEB TF37.9 E6.7 S1.74 W146 L
MAR TF44.4 E7.9 S3.34 W148 F.7 L
APR TF46.4 E7.4 S6.18 W130 F.7 L
MAY TF53.9 E10.5 S5.16 W132 F.8 L
JUN TF58.3 E12.4 S5.41 W145 F.8 L
JUL TF58.7 E13.1 S4.91 W152 F.8 L
AUG TF60.0 E14.3 S4.91 W122 F.8 L
SEP TF57.0 E12.8 S5.67 W150 L
OCT TF55.0 E12.7 S3.09 W170 L
NOV TF45.9 E9.5 S1.87 W151 L
DEC TF44.5 E8.6 S1.72 W184 L
Z

```

TF mean daily air temperature °F  
 E mean daily vapour pressure millibars  
 S mean daily sunshine hours  
 W mean daily wind speed, miles per day  
 F seasonal factor  
 L Data complete

FIGURE 1—SPECIMEN OF DATA AS PUNCHED ON PAPER TAPE

```

21/12/61--22                                     Date and serial number of calculation
PENMAN EVAPORATION RATE PROGRAMME.             Title of Programme

```

```

UXBRIDGE YEAR 1954                               Title copied from data tape

```

```

+0.2
+0.5
+1.3
+2.5
+3.1
+3.7
+3.6
+2.8
+2.2
+1.0
+0.3
+0.2

```

+0.9  
 +1.7  
 +2.5  
 +3.0  
 +2.9  
 +2.3

f.E<sub>0</sub> millimetres per day

E<sub>0</sub> millimetres per day

FIGURE 2—SPECIMEN OF RESULTS CALCULATED FROM DATA SHOWN IN FIGURE 1

A detailed specification of the programme which shows the conventions to be observed in punching the data and in altering the constants, is available at the Road Research Laboratory.

**Acknowledgments.**—The author wishes to thank Dr. H. L. Penman for useful comments and suggestions on the preliminary proposals and specification of this programme.

The computer programme described in this article was prepared as part of the programme of the Road Research Board of the Department of Scientific and Industrial Research. The article is published by permission of the Director of Road Research.

## REFERENCES

1. PENMAN, H. L.; Natural evaporation from open water, bare soil and grass. *Proc. roy. Soc., London*, **193**, 1948, p. 120.
2. PENMAN, H. L.; Woburn irrigation 1951-59, 1. Purpose, design and weather. *J. agric. Sci., Cambridge*, **58**, Pt. 3, 1962, p. 343.
3. KAYE, G. W. C. and LABY, T. H.; Tables of physical and chemical constants and some mathematical functions. 12th edn, London, Longmans, Green and Co., 1958.

551.515.82:551.543.5:532.59

## AN OSCILLATORY PRESSURE JUMP AT MALTA

By T. H. KIRK

Examples have already been given<sup>1</sup> of pressure jumps at Malta. Most of them have been characterized by oscillations in the wind and pressure records after the initial sharp rise of pressure. A particularly good example of an oscillatory pressure jump occurred just after 0100 local time (GMT + 1 hr) on 6 September 1960 (Figures 1 and 2). The marked periodicity in the wind speed trace was particularly evident, even when the periodicity in the direction trace had largely disappeared.

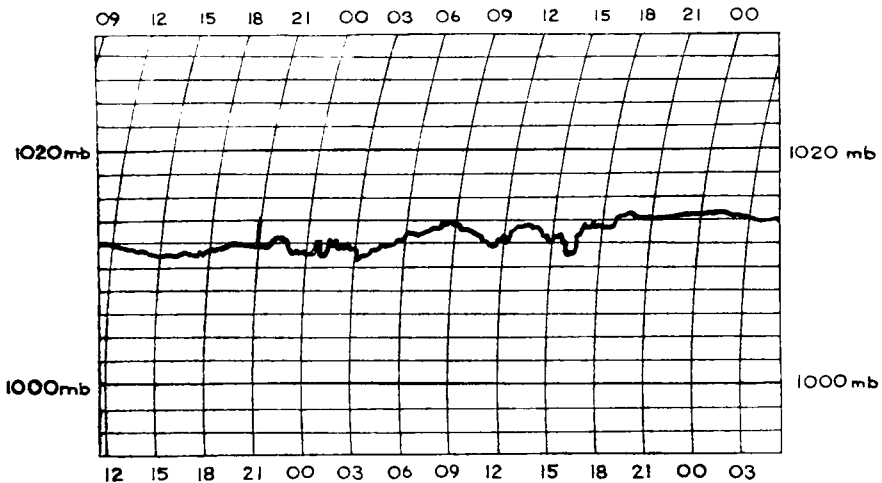


FIGURE 1—BAROGRAM FOR LUQA, MALTA, 6 SEPTEMBER 1960

Goldie<sup>2</sup> has dealt with the effects at the surface attributable to waves at an approximately horizontal surface of discontinuity in the atmosphere, and it may be of interest to quote his remarks when deriving the variation vector ( $\delta U$ ) of the surface wind:

“It is a matter of much interest that, even in cases where the surface wind may have dropped to calm at night, this  $\delta U$  effect is strikingly evident in the form of a little breeze rising steadily to a maximum and then dying out in the same way at the appropriate times.”

The wind record can be interpreted in much the same way, for after 0300 local time the surface wind was very light and yet the periodicity remained

particularly evident in the speed. The 0001 GMT Qrendi ascent shows that the height of the inversion was at approximately 350 feet above station level at Luqa. The 1200 GMT ascent shows that the inversion had increased in height by 30 mb, i.e. approximately 900 feet, so that if we could assume that the whole of this increase took place at the pressure jump we should have a height of about 1250 feet for the inversion at Luqa.

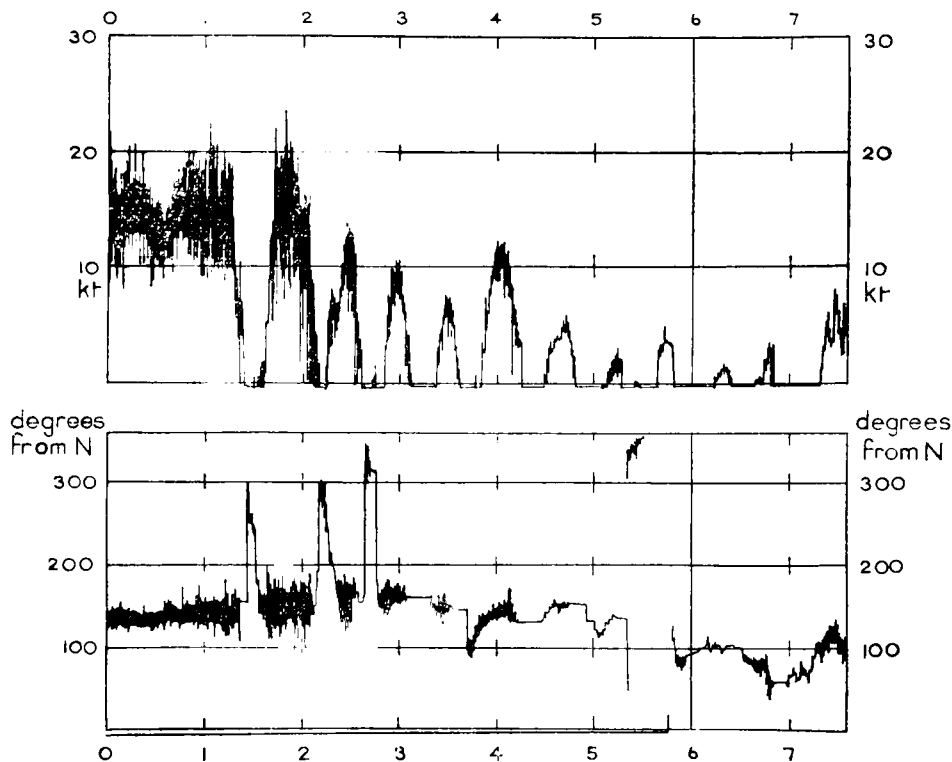


FIGURE 2—ANEMOGRAM FOR LUQA, MALTA, 6 SEPTEMBER 1960

Figure 3 shows the synoptic situation at the surface at 0001 GMT, a discontinuity line being drawn along the trough. If we take the orientation of this line as  $030-210^\circ$  at Malta then we should expect the pressure jump to arrive from the direction  $(210+90)^\circ$ , i.e. from  $300^\circ$  approximately. At the onset of the sharp pressure rise there would be no geostrophic equilibrium and the surface wind would blow at right-angles to the pressure jump line, i.e. from approximately  $300^\circ$ . This is in accordance with the first three swings of the wind direction. After 0300 local time, if the direction of the waves be taken at right-angles to the trough line, the observations are consistent with a mean wind ( $U$ ) of approximately 5 knots from  $140-150^\circ$  and a variable vector ( $\delta U$ ) of 5 knots. The surface wind would then be varying between  $140^\circ$  and  $150^\circ$  10 knots and zero as the observations confirm.

Using the value of  $\delta U$  in the formulae given by Goldie, we obtain 10 knots for  $v$ , the speed of the waves relative to the component of the surface wind in the direction of the waves. The wind is out of phase with the pressure variations for we note that the first sharp decrease of wind is due to the pressure jump.

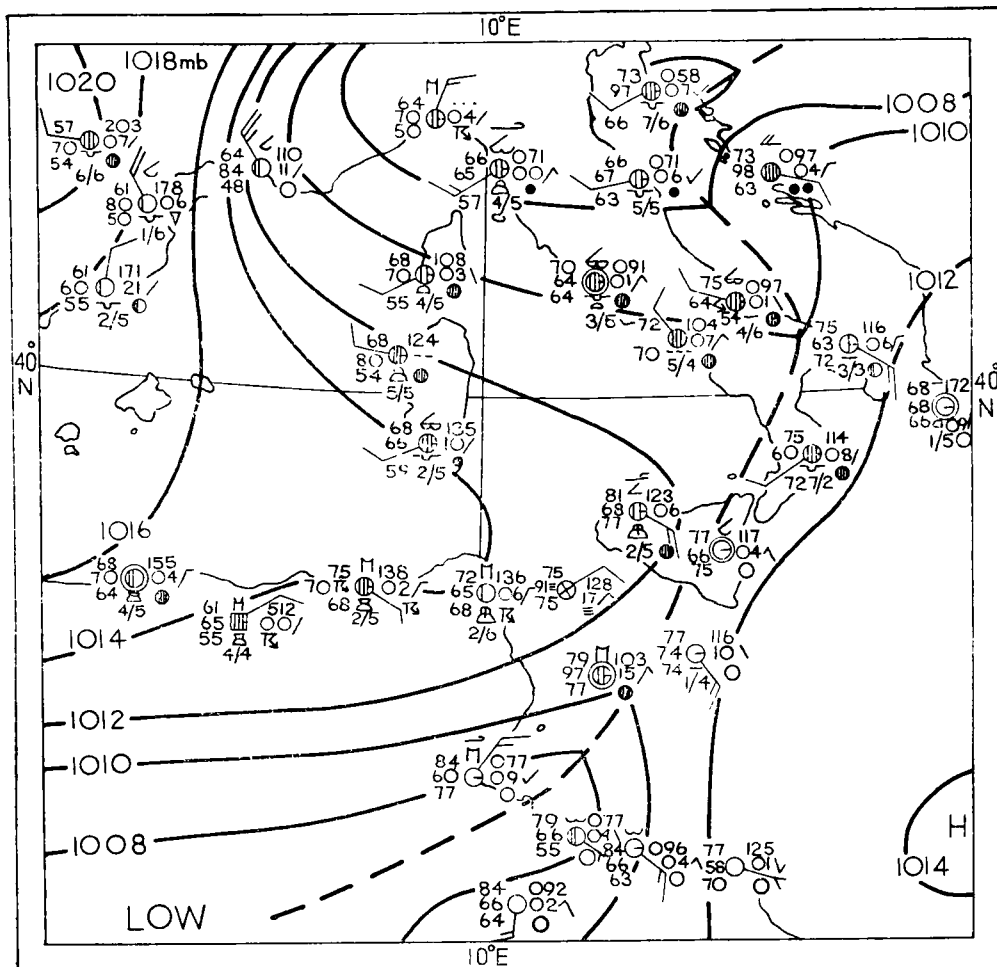


FIGURE 3—SURFACE CHART FOR 0001 GMT, 6 SEPTEMBER 1960

We have, therefore, in Goldie's notation

$$\begin{aligned}
 U \cos \alpha - V &= +10 \text{ knots} \\
 U \cos \alpha &= 5 \text{ knots approximately} \\
 \text{therefore } V &= -5 \text{ knots}
 \end{aligned}$$

i.e. the waves are from the north-west at a speed of about 5 knots.

The period of the waves shown by the anemogram is about 40 minutes. Using this fact we derive 120 metres for the wavelength. The amplitude of the waves comes to somewhere between 200 feet and 600 feet depending on the assumed height of the inversion. These simple computations have of course only limited application because the surface wind is not entirely representative of the layer of air below the inversion.

It is of interest to note that Tepper<sup>3</sup> has referred to oscillatory pressure jumps and has cited experimental evidence that hydraulic jumps are oscillatory when  $h_2/h_1 < 2$ ,  $h_1$  and  $h_2$  being the heights of the bottom layer before and after the jump. Owing to the uncertainty in the height of the inversion immediately after the pressure jump it is difficult to know whether or not this criterion was

satisfied in this instance. However, even assuming that the 1200 GMT value of the inversion height was applicable at the jump, we have, reckoning from sea level,

$$\frac{h_2}{h_1} = \frac{1550}{650} = 2.4 .$$

Experience in the Mediterranean does undoubtedly support the idea that weak pressure jumps are oscillatory.

#### REFERENCES

1. KIRK, T. H.; Pressure jumps at Malta. *Met. Mag., London*, **90**, 1961, p. 206.
2. GOLDIE, A. H. R.; Waves at an approximately horizontal surface of discontinuity in the atmosphere. *Quart. J. R. met. Soc., London*, **51**, 1925, p. 239.
3. TEPPER, M.; The application of the hydraulic analogy to certain atmospheric flow problems. *U.S. Dept. of Commerce, Weather Bureau Res. Pap., Washington*, No. 35, 1952.

551.509.317:551.509.326

### A MODIFIED INSTABILITY INDEX

By G. J. JEFFERSON, M.Sc.

The instability index for the months May to August in the British Isles and near continental areas described by Rackliff<sup>1</sup> possesses the very desirable features for a forecasting tool of simplicity and quick computation. Some attempt has been made at London (Heathrow) Airport to use it in midsummer, especially in regard to air-mass thunderstorm activity, and to ascertain the possibility of its application to wider areas. While no comprehensive investigation of its value has so far been possible, one or two features have come to light which suggest that some modification is necessary for it to be used in this way.

On one occasion the instability index ( $\Delta T$ ), for an area covering all radio-sonde stations of the North Atlantic from Bermuda to Greenland, the British Isles and the eastern half of Canada and the United States of America, was highest (34) at Ocean Weather Station "A" (62°N 33°W), in an area of ocean where thunderstorms are almost unknown, while in a thundery area south-west of New York the index was about 29. A number of trials have also been made over the Europe-Mediterranean area. One example of this is given in Figure 1. It will be noted that this chart is based on the ascents for 1200 GMT in place of the midnight ascents used by Rackliff, and would be expected to show a closer coincidence to actual thunderstorm occurrence since the effects of advection are reduced. Isoleths of  $\Delta T$  show areas of maximum over Spain, northern Italy to Yugoslavia with a northward extension towards north-west Germany and other areas near western Ireland and over Scandinavia. Also on Figure 1 are plots of rain, showers and thunderstorms for 1500 GMT on the same day. These show that the southern areas of maximum  $\Delta T$  coincided fairly well with the areas where thunderstorms occurred but that nothing heavier than showers was reported from the northern area of maximum. SFLOC reports for 1500 and 1600 GMT covered fairly wide areas of continental Europe south of 50°N but there were no reports north of 50°N. These facts suggest that there will be a higher threshold value for thunder in cold than in warm air and that some modification is necessary to the method of evaluation if the index is to be used over greater ranges of temperature (or latitude) than those for which it was evolved, or indeed if it is to be used at other seasons in north-west Europe.

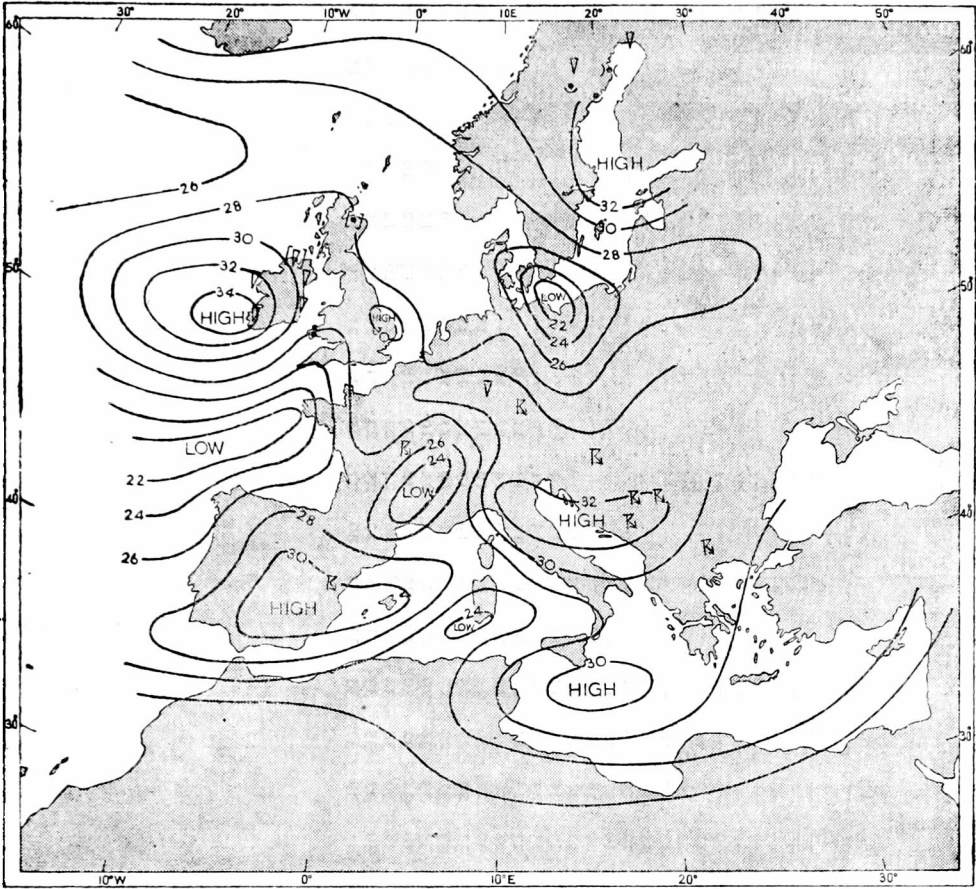


FIGURE 1—ISOPLETHS OF INSTABILITY INDEX ( $\Delta T$ ) AFTER RACKLIFF  
FOR 1200 GMT, 18 JUNE 1962

Present weather plots at 1500 GMT. Plots of weather in past hour are in square brackets.

The instability index  $\Delta T$  is a number of only relative significance, and, unlike the index of Showalter,<sup>2</sup> its magnitude will in fact depend not only on the stability but also on temperature. This is readily apparent if saturated air with a lapse rate equal to the saturated adiabatic between 900 and 500 mb (that is, constant wet-bulb potential temperatures,  $\theta_w$ ) is considered. The following table shows how  $\Delta T$  varies with  $\theta_w$  in this case.

TABLE I—RELATIONSHIP BETWEEN  $\Delta T$  AND  $\theta_w$

$\theta_w$ °C	$T_{500}$ °C	$\Delta T$
0	-41	41
5	-33	38
10	-26	36
15	-17	32
20	-9	29
25	-1	26

It can be seen that as  $\theta_w$  rises, the instability index for air of neutral stability falls steadily. Values of  $\theta_w$  between 10°C and 20°C would be fairly typical of air over north-west Europe in the summer months which was used by Rackliff to evaluate the threshold value of  $\Delta T$  to give thunderstorms. The corresponding variation of  $\Delta T$  in Table I is between 36 and 29. Since actual soundings resembling the air used to evaluate Table I are of the type usually associated



with convectational activity, the threshold value of  $\Delta T = 30$  for thunderstorms given by Rackliff can be seen to be reasonable. Table I shows that  $\Delta T$  would have a value of 30 when  $\theta_w \simeq 18^\circ\text{C}$ . Also the change of  $\Delta T$  with  $\theta_w$  is approximately linear and it is suggested that the following amended formula based on the data in Table I will give a value of the instability index which is independent of temperature and which will still give the same threshold value for thunderstorms over a wide range of temperature:

$$T_J = 1.6 \theta_{w900} - T_{500} - 11$$

where  $T_J$  = the amended thunderstorm index,  $\theta_{w900}$  = 900 mb wet-bulb potential temperature and  $T_{500}$  = dry-bulb temperature at 500 mb. With saturated air of neutral stability this gives a value of  $T_J = 30$  when  $\theta_w = 18^\circ\text{C}$ , a typical value for summer thunderstorm conditions over the British Isles. Figure 2 shows isopleths of  $T_J$  for the same occasion as Figure 1 and it is evident that the northern maximum is now much less prominent.

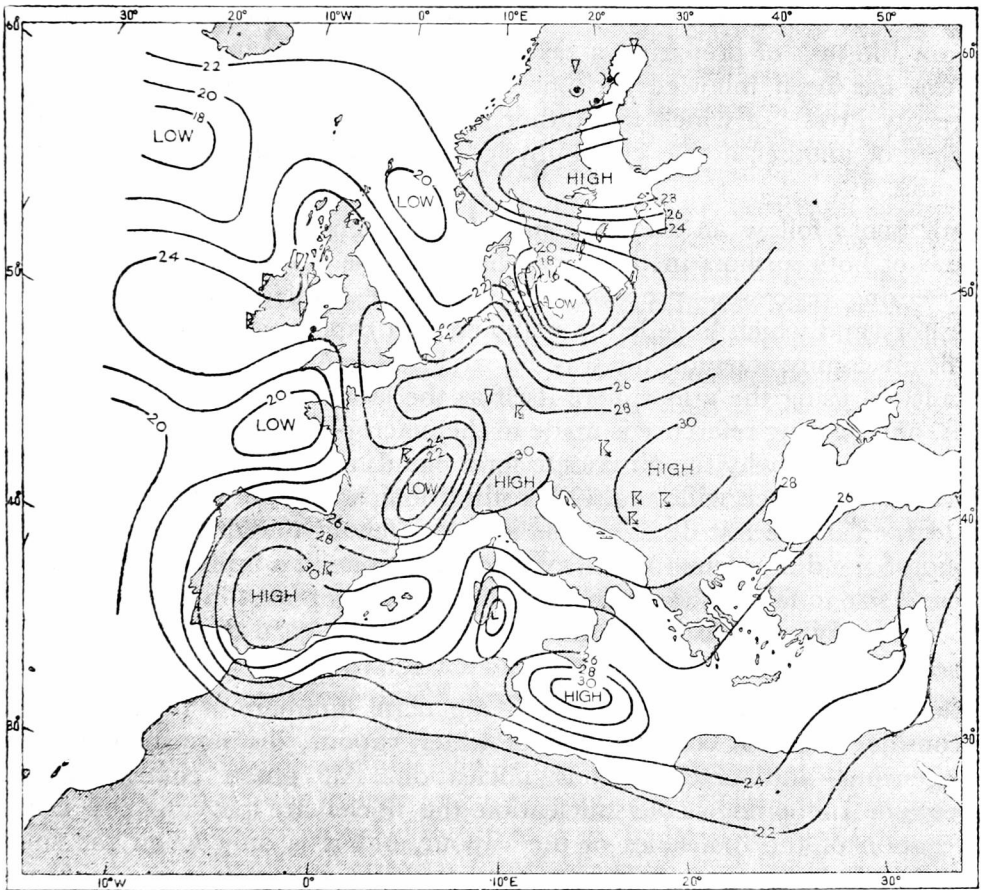


FIGURE 2—ISOPLETHS OF MODIFIED INSTABILITY INDEX ( $T_J$ ) 1200 GMT, 18 JUNE 1962

Present weather plots at 1500 GMT. Plots of weather in past hour are in square brackets.

By the introduction of this altered formula some of the speed of evaluation is lost. Table II is therefore intended to overcome this. It shows values of  $T_J$

for ranges of  $\theta_{w900}$  and  $T_{500}$  which would cover most normal requirements and can be used to evaluate the modified instability index as quickly as in the original case.

#### REFERENCES

1. RACKLIFF, P. G.; Application of an instability index to regional forecasting. *Met. Mag., London*, **91**, 1962, p. 113.
2. SHOWALTER, A. K.; A stability index for thunderstorm forecasting. *Bull. Amer. met. Soc., Lancaster, Pa.*, **34**, 1953, p. 250.

551.574.1(048.1)

### THE PHYSICS OF RAINCLOUDS

By R. F. JONES, B.A.

The deceptively simple question of "how does it rain?" has led the meteorologist interested in the physics of clouds into increasingly complicated fields of study, the difficulties and range of which have been recently recognized by the creation of a professorship in cloud physics at Imperial College, University of London. The first holder of this chair, Professor B. J. Mason, was the first to attempt the task of preparing a textbook on this advancing subject in 1957<sup>1</sup> and this has been followed in 1962 by a further textbook\* (from the rival University Press), of which the author is Dr. N. H. Fletcher, until recently a member of another active cloud-physics group led by Dr. E. G. Bowen in Australia.

Both books follow an almost identical approach which reflects the prime interest of both authors in the microphysics of the condensation, sublimation and freezing processes—processes which can be studied individually in the laboratory and which have led to many elegant experiments. It is, however, a significant commentary on the way research has gone, and a reflexion of the difficulty of using the atmosphere itself as the laboratory, that, again in both books, only passing reference is made to the macrophysics or dynamics of cloud systems, how and why the air rises to form clouds and how quickly, so that the question "how much will it rain?" is still a long way from solution. What we *have* learned in the last decade or so is how a few favoured droplets among a myriad of cloud droplets—on the average about one in a million—can grow to sufficient size to fall to the ground as rain. The story makes interesting reading and we can follow in brief outline Dr. Fletcher's logical development of the theme.

After a brief chapter, which is really a general summary of the whole book, we consider first the condensation of water vapour, distinguishing between homogeneous and heterogeneous nucleation. All phase changes require nucleation. In homogeneous nucleation the nuclei are provided by chance aggregation of the molecules of the vapour, and it is only when the supersaturation is large that such aggregates last long enough and are formed sufficiently frequently to have a chance of further growth into droplets. In heterogeneous nucleation, condensation gets off to a good start by using particles of foreign material as a framework to which molecules of the vapour can attach themselves, so that the embryo droplet is more readily formed at a much lower supersaturation. Because the atmosphere always contains airborne

---

\* *The physics of rainclouds*, by N. H. Fletcher. 9in. x 5½in., pp. x + 386, *illus.*, London, Cambridge University Press, Bentley House, 200 Euston Road, London, N.W.1, 1962. Price: 65s.

foreign particles, the process of heterogeneous nucleation is the atmospheric condensation process and water-vapour supersaturation never becomes large. The theory of nucleation is complex but Dr. Fletcher's chapter takes us carefully through from homogeneous nucleation to nucleation by ions and to nucleation by insoluble and soluble particles, with the effects of the structure of the particles. By the end of the chapter we are convinced that the particles that really matter in atmospheric condensation processes are relatively large and preferably soluble, and that homogeneous nucleation of the liquid phase and condensation on ions have no part to play in nature. What we mean by "relatively large" in this context becomes clearer in the next chapter when the naturally occurring nuclei are considered.

An enormous amount of observational work has gone into the collection of nuclei of all the sizes which occur in the atmosphere. Many of the determinations have relied on an expansion chamber, a method which produces high supersaturation not typical of the free atmosphere, so that many of the nucleus counts have no relevance to cloud physics but are really measures of the total nucleus concentration. This total concentration is enormously variable, the average per cubic centimetre ranging from about 1000 in air near the tops of high mountains and over the oceans to about 100,000 in city air, but only the larger hundred or two hundred of these take any part in condensation processes and measurements have shown these to have radii of  $0.1\mu$  or greater. These are referred to as "large" nuclei while "giant" nuclei, which are composed mostly of sea-salt, have radii greater than  $1\mu$ . Much is made here, and later in the book, of the difference between continental and maritime clouds which is traced to a basic difference in nuclei; the continental air has more of the efficient "large" condensation nuclei than maritime air and therefore a greater concentration of droplets when cloud is formed.

Having decided which nuclei are important in the formation of cloud, the author next considers the cloud droplets themselves, which are formed on the nuclei, and the methods used to determine droplet concentrations and size-distributions together with their integrated effect (total liquid-water concentrations) in cloud. The general shape of droplet distribution curves, when number concentration is plotted against drop radius, is bell-shaped but generally asymmetrical with a tail extending towards large radii. Clouds which show no tendency to develop rain have a narrow spread of droplet sizes while the clouds which ultimately give rain have a large spread. This is claimed as a distinguishing feature between cumulus clouds found in continental air and those found in maritime air, the former with a narrow droplet spectrum showing less tendency to rain for a given cloud thickness than the latter which have a wider spectrum. How difficult it is to get a broad spectrum of droplet sizes by condensation alone is shown by the theoretical calculations of the next chapter from which it is learned that, because in the initial stages of condensation the smaller particles grow much more rapidly than the larger, condensation alone leads to a narrowing of the drop-size spectrum.

One of the processes which might widen the size spectrum of droplets is coalescence between droplets and this is next considered. Coalescence between droplets having radii less than  $18\mu$  has been shown both theoretically and in

practice to be unlikely, but larger droplets can sweep up the droplets in their path as they fall with an efficiency which increases as their size increases. This process can be used to explain the fact that rain falls on occasions from non-freezing clouds and the theoretical arguments, using somewhat idealized conditions, support this conclusion by showing that the times of growth of droplets to raindrop size are reasonable. It is an interesting demonstration of the development of ideas of rain-producing mechanisms, even in the last 15 years, to find this chapter commence "The fact that rain can fall from clouds whose temperatures are everywhere warmer than freezing is now sufficiently well known to require no documentation", but the reference to radar, which has contributed notably in providing evidence for this assertion, is disappointingly perfunctory.

The other powerful mechanism leading to the formation of rain, and probably the only one in extensive clouds where up-currents are gentle, involves the ice-phase and is usually known as the Bergeron process. This basic theory relies on the fact that the saturation vapour pressure over ice is less than that over supercooled water at the same temperature. An ice crystal in the presence of supercooled water droplets is therefore in an environment which is supersaturated and grows rapidly while the droplets evaporate in the endeavour to maintain saturation with respect to water. If the ice crystals are relatively few they will grow quite large and will acquire a fall-speed large compared with that of the droplets, so that they will also grow by accretion of droplets as they fall, finally melting to raindrops as they descend below the melting level. All this has been known in outline for some time, but, as Dr. Fletcher shows, the details of the production of the original ice crystals are still obscure. Ice crystals do not form at all readily in the atmosphere at temperatures higher than about  $-15^{\circ}\text{C}$ , either by the freezing of droplets or by direct sublimation, and, without the presence of suitable nuclei, would probably not form at all until temperatures fell below about  $-40^{\circ}\text{C}$  (homogeneous nucleation). The theories of homogeneous and heterogeneous nucleation of ice from the water or vapour phase are similar in principle to those of nucleation of water from the vapour phase, but the surface structure of the nucleus assumes a greater importance. Experiments show that, if a given volume of air is cooled, more and more nuclei become active as freezing nuclei but little is known about the chemical composition and origin of these particles except that they are probably solid and insoluble. Laboratory experiments with different mineral dusts have given a variety of threshold temperatures and it is thought that most naturally occurring freezing-nuclei originate at the earth's surface. The book contains a carefully reasoned discussion of Bowen's meteor-dust hypothesis resulting in a verdict of "non-proven". A few substances, which do not occur naturally in any quantity, have a crystal structure so similar to ice that they might be expected to be efficient as ice-forming nuclei. This has in fact been shown to be true and the most efficient of these, which can produce a few ice crystals at temperatures as high as  $-4^{\circ}\text{C}$  and vastly more as temperatures decrease, is silver iodide. Following the discovery of a simple way of dispensing silver iodide in finely divided form, as a smoke from a burner, this substance has achieved notoriety from its use in attempts to increase rainfall. This and other methods of modifying clouds are discussed realistically in the last three chapters of the book. No support is given to exaggerated claims, and the great difficulties of verification

of any effect are stressed. It is here that the lack of knowledge of the dynamics of cloud systems is most felt; for if we cannot say how much it will rain naturally in a given situation, how can we say whether an increase in rainfall has been achieved?

The book is clearly written and well produced with a few minor errors only and, although the advances it has to report since Mason's book was written are few and the general approach is similar, there is always room among textbooks for one of this quality.

#### REFERENCE

1. MASON, B. J.; *The physics of clouds*. Oxford, Clarendon Press, 1957.

#### REVIEW

*Microcards of IGY meteorological data*, by G. London. 9½ in. × 6¼ in., pp. x + 78, *illus.*, World Meteorological Organization, Geneva, 1962. Price: Sw. fr. 7.—.

The present virtual completion of the task of reproducing meteorological data of the International Geophysical Year (IGY) on microcard affords an opportune time for this report by Dr. G. London, Chief of the IGY Meteorological Data Centre of the WMO Secretariat, to place on record some of the problems of collection, cataloguing, storage and publication difficulties inevitably encountered with some seven million synoptic surface and upper air observations.

It is emphasized in the introductory remarks that the main underlying principle which determined the basic arrangement of the microcards was the fact that such unique records should be prepared and devised in such a way that any of the observations could be traced quickly and easily. Naturally the procedures chosen were determined to some extent by the characteristics of the material collected, and the first chapter gives a brief description of the WMO standard forms that were used and compiled by the participating meteorological services.

With such an unprecedented programme of scientific observations, a careful registering of incoming forms was imperative, and Chapter II concisely shows that the system should constitute a complete, reliable and permanent record of information which, even after the termination of the IGY, could still be used to trace and retrieve the original observations.

After a small section considering the complementary problem of storage, the final chapter is devoted to the major difficulties concerning the actual publication of the data.

In more detail it is shown that a complete set of microcards for the IGY period was made to consist of four parts corresponding to the WMO standard forms, the basic layout being in terms of (i) type of observation (ii) geographical region and (iii) chronological period.

Here again we see that the report considers the danger in the use of unconnected classifying principles which in themselves would defeat their own purpose. Only by a system that was based on a classification scheme embodying the characteristics of the material itself, could the data be readily accessible, each microcard being identifiable by a combination of two groups of three numerals indicating type of form and synoptic hour with the appropriate pentad code.

The volume is concluded by the inference that individual microcard reference numbers constitute, at the same time, a classification system for the whole of the synoptic meteorological data published on microcards and will serve as guides for filing and information retrieval. It is significant that the system was adaptable enough for the International Geophysical Co-operation reports (1959) to be grouped and coded by the same principles of layout and notation.

The information supplied will be of considerable interest to the users of microcards and the principles formulated will, no doubt, find a use in any future projects of a similar nature.

J. F. DIXON

### OBITUARY

*Mr. D. H. Clarke.*—It is with great regret that we record the sudden death on 14 January, 1963, at the age of 60, only seven months following his retirement, of Mr. D. H. Clarke, Senior Experimental Officer. It was on 17 December 1926, that Duggie joined the Meteorological Office at Aldergrove as a Temporary Clerk, having had previous experience in meteorological work while serving in the Royal Air Force in Iraq. He remained at Aldergrove until the early 1930's when moves entailed service at Croydon, Headquarters, Birmingham and Dunstable. From early 1940 and throughout the war years he was in charge of the training of W.R.A.F. Meteorologists in London and at Stonehouse. In 1948 he returned to Dunstable on appointment in charge of the Administrative Branch and occupied this post until his retirement in June 1962.

Duggie had a great charm of manner and his many friends both in the Meteorological Office, Works Services Officers with whom he had many contacts while at Dunstable and also his numerous local friends, will feel regret that he did not live longer to enjoy retirement. Among the outside interests in which he took an active part was membership of the South Bedfordshire Preservation Society and the Manshead Archaeological Society. He was keen on outdoor life and the country while indoor hobbies included woodwork at which he was most efficient and artistic.

To his widow and son, now employed by Shell Mex in the Persian Gulf as a Geologist, his friends and colleagues offer deepest sympathy in their sad loss.

A.A.V.B.

### METEOROLOGICAL OFFICE NEWS

The Meteorological Office Football Club (Bracknell) having received a bye in the first round, safely entered the third round of the Lewis Cup when they beat Cheltenham Civil Service A.F.C. by 7 goals to 3 on 28 November. Although a goal down inside two minutes, the team fought back to be 3 - 1 in the lead at half-time and were worthy winners of a good, exciting game.

The goalscorers were Archard, Underwood 3, Johnson 2, own goal 1 and the team was Robinson (Heathrow); Crisford (White Waltham), Saunders (M.O. 5c); Hanson (M.O. 18), Rattray (M.O. 3), Green (M.O. 10); Morgan (M.O. 18), Underwood (M.O. 5c), Johnson (Heathrow), Ashby (M.O. 15) and Archard (M.O. 3). The Club is grateful to the Director-General of the Meteorological Office for agreeing to have the teams presented to him before the kick-off and to the many other members of the staff who supported the team. The team will now be meeting Portsmouth Civil Service A.F.C. for the right to enter the last eight in the competition.